The 16th Workshop on QCD Phase Transition and Relativistic Heavy-Ion Physics (QPT 2025)

Connections between heavy-ion Collisions and EIC/UPC

Wenbin Zhao
Central China Normal University
Oct. 24 – 28, 2025, Guilin, China

UPC/DIS and Heavy-ion Collisions

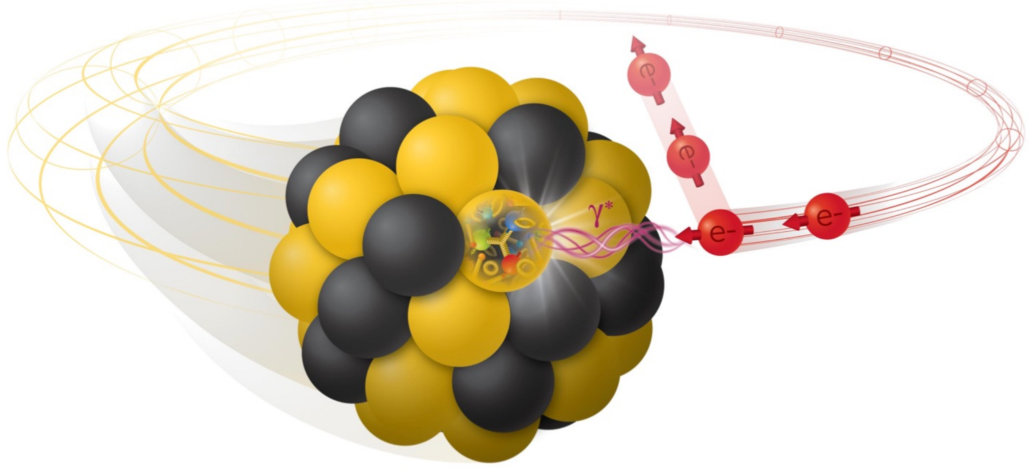

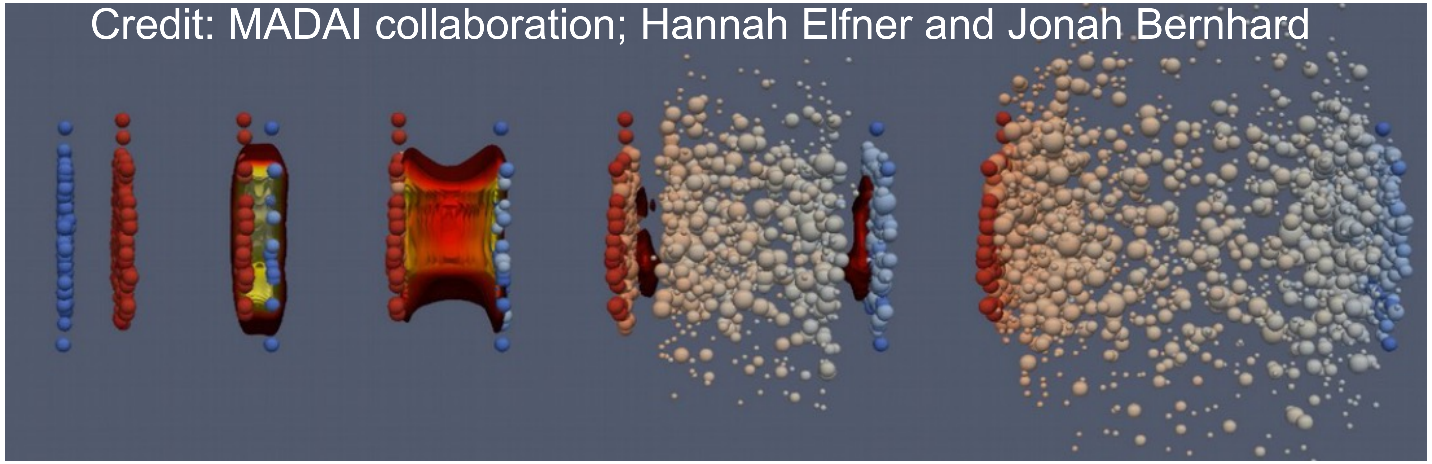

- **UPC/DIS:**
- Pin down kinematics, clean probes of QCD dynamics
- Collision energy is limited.

- **Heavy-ion Collisions:** High center-of-mass energies available.
- **Multi-Stage process:**

Initial state => QGP => Hadronic Scatter

- It is the same nucleus at small x: probe the initial state in UPC/DIS, then apply to heavy ion simulations.

Imaging nuclei with photon-nucleus reactions

High energy factorization:

1. $\gamma^* \to q\bar{q}$ splitting, wave function $\Psi^\gamma(r, Q^2, z)$
2. $q\bar{q}$ dipole scatters elastically N(r, x, b)
3. $q\bar{q} \to J/\Psi$, wave function $\Psi^V(r, Q^2, z)$

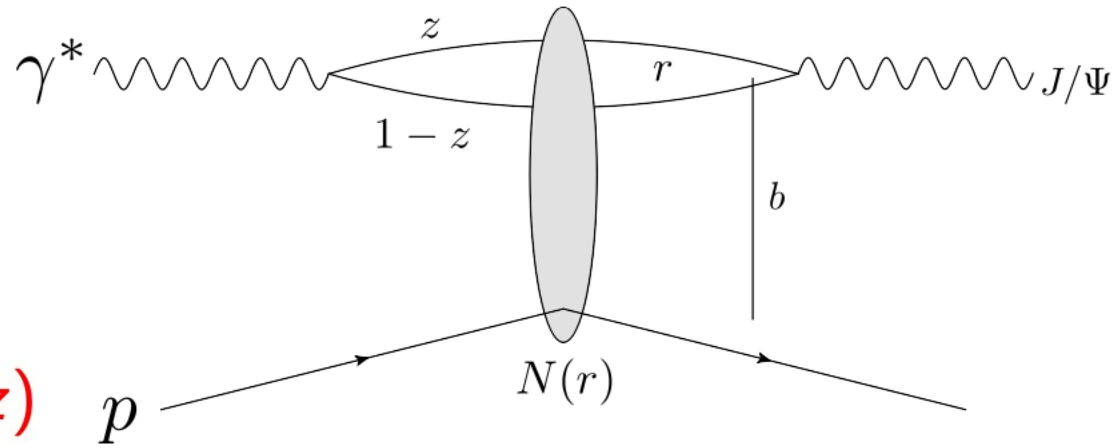

Diffractive scattering amplitude

$$\mathcal{A}^{\gamma^* p \to Vp} \sim \int \mathrm{d}^2 b \mathrm{d}z \mathrm{d}^2 r \Psi^{\gamma *} \Psi^V (r, z, Q^2) \mathbf{e}^{-i\mathbf{b}\cdot\mathbf{\Delta}} N(r, x, b)$$

Impact parameter, b, is the Fourier conjugate of the momentum transfer, $\Delta \approx \sqrt{-t}$

N(r, x, b) dipole-target scattering amplitude.

Miettinen, Pumplin, PRD 18, 1978; Caldwell, Kowalski, 0909.1254; Mäntysaari, Schenke, 1603.04349; Mäntysaari, 2001.10705

Imaging nuclei with photon-nucleus reactions

High energy factorization:

1. $\gamma^* \to q\bar{q}$ splitting,
   wave function $\Psi^{\gamma}(r, Q^2, z)$
2. $q\bar{q}$ dipole scatters elastically N(r, x, b)
3. $q\bar{q} \to J/\Psi$, wave function $\Psi^{V}(r, Q^2, z)$

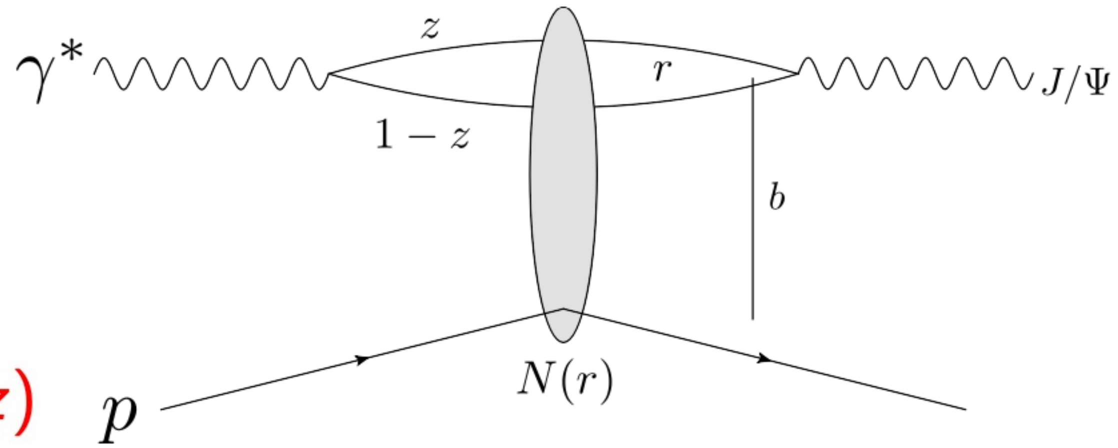

Diffractive scattering amplitude

$$\mathcal{A}^{\gamma^* p \to Vp} \sim \int \mathrm{d}^2 b \mathrm{d}z \mathrm{d}^2 r \Psi^{\gamma *} \Psi^{V}(r, z, Q^2) \mathbf{e}^{-i\mathbf{b}\cdot\boldsymbol{\Delta}} N(r, x, b)$$

Impact parameter, b, is the Fourier conjugate of the momentum transfer, $\Delta \approx \sqrt{-t}$
N(r, x, b) dipole-target scattering amplitude.

A ~Fourier transform of the spatial structure function of target ($T_{p/A}$).

Miettinen, Pumplin, PRD 18, 1978; Caldwell, Kowalski, 0909.1254; Mäntysaari, Schenke, 1603.04349; Mäntysaari, 2001.10705

Coherent and incoherent processes

- **Coherent** $\sigma_{\text{coherent}} \sim |\langle \mathcal{A} \rangle_\Omega|^2$

Target stays intact, (|initial state> = |final state>)
Probes the average shape of the target.

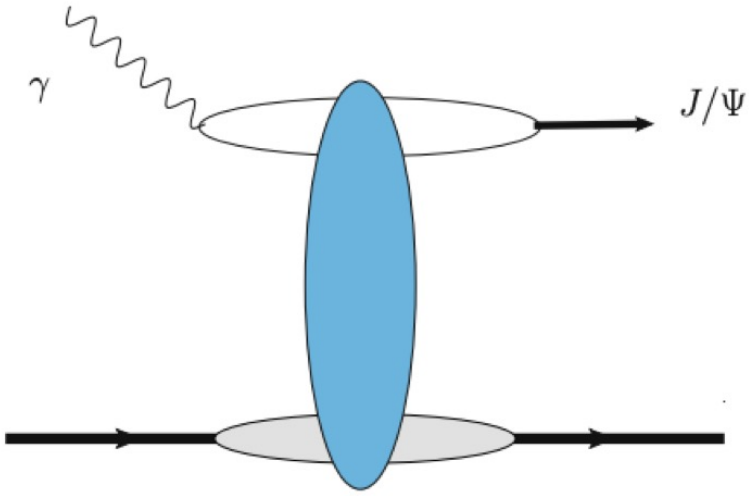

Miettinen, Pumplin, PRD 18, 1978; Caldwell, Kowalski, 0909.1254; Mäntysaari, Schenke, 1603.04349; Mäntysaari, 2001.10705

Coherent and incoherent processes

- **Coherent** $\sigma_{\text{coherent}} \sim |\langle \mathcal{A} \rangle_\Omega|^2$

Target stays intact, (Iinitial state> = Ifinal state>)
Probes the average shape of the target.

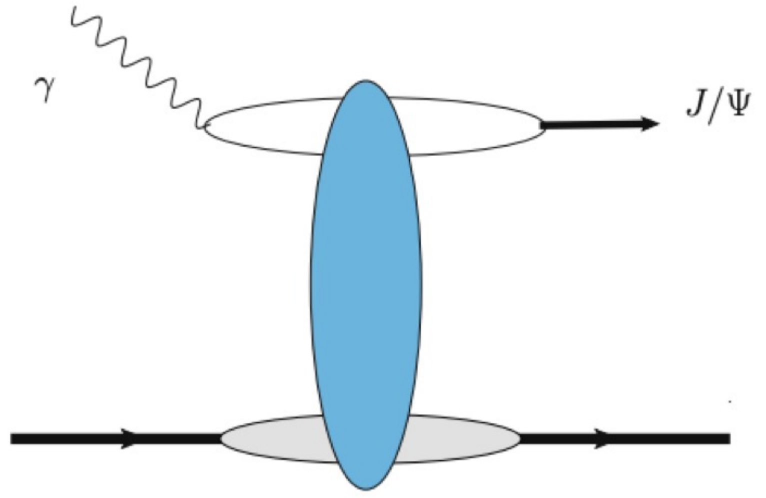

- **Incoherent** $\sigma_{\text{incoherent}} \sim \langle |\mathcal{A}|^2 \rangle_\Omega - |\langle \mathcal{A} \rangle_\Omega|^2$

Target breaks apart, (|initial state> ≠ |final state>)

Probes the variance of event-by-event initial state fluctuations in target structure.

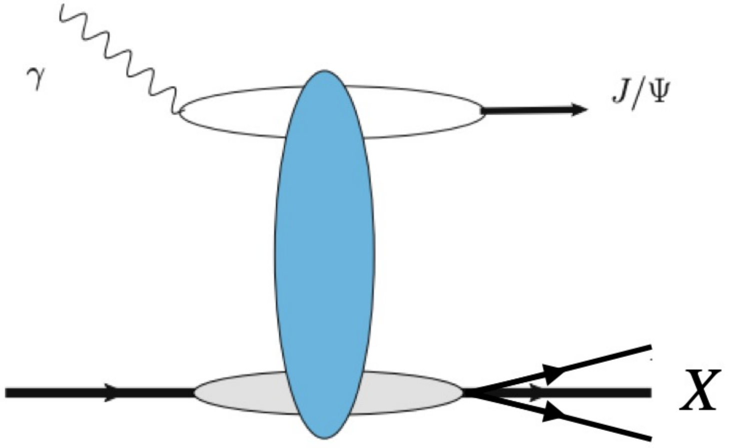

Miettinen, Pumplin, PRD 18, 1978; Caldwell, Kowalski, 0909.1254; Mäntysaari, Schenke, 1603.04349; Mäntysaari, 2001.10705

Proton geometry fluctuations

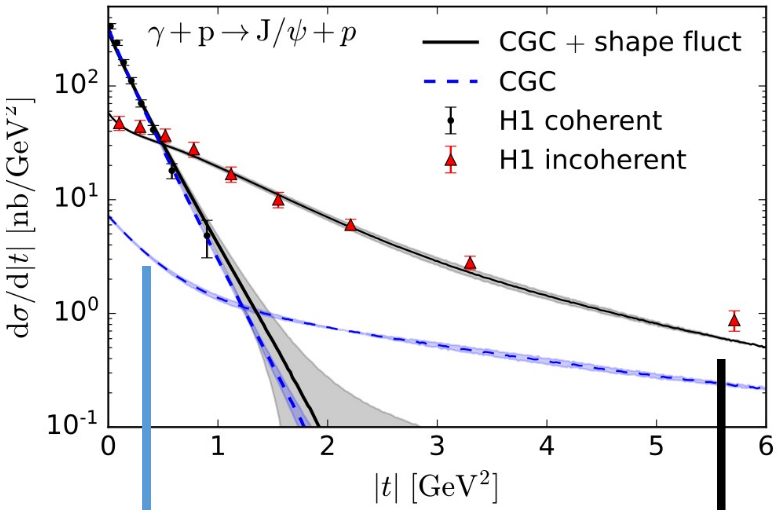

No subnucleon fluctuations

With subnucleon fluctuations

- Probe the event-by-event sub-nucleon fluctuations.

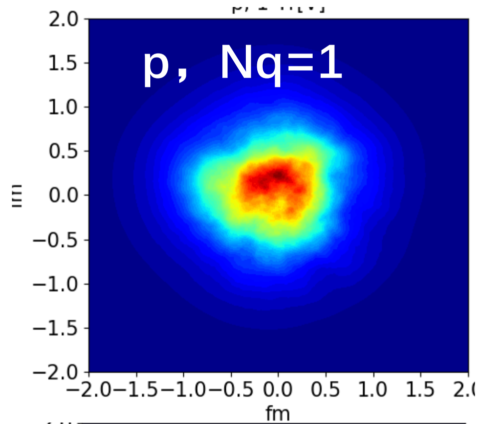

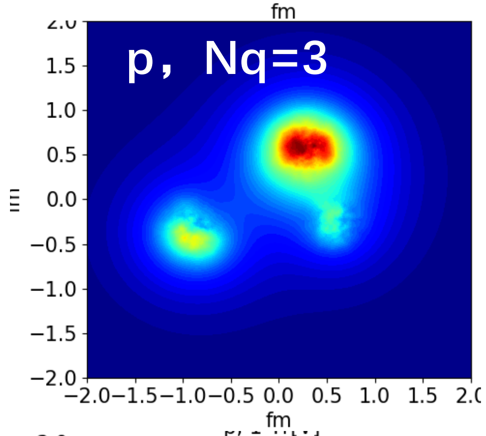

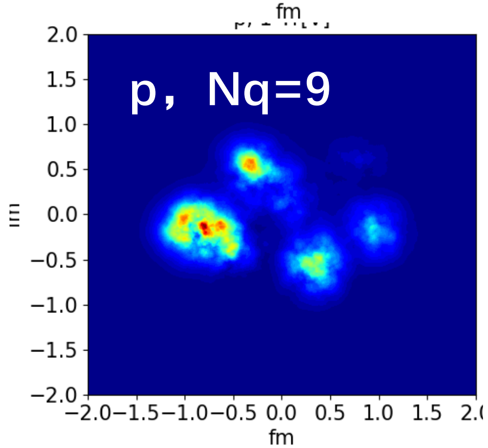

H. Mäntysaari, Schenke , PhysRevLett.108.252301 , PhysRevC.86.034908 ;
H. Mäntysaari, F. Salazar and B. Schenke, Phys. Rev. D 106, 074019 (2022).
H. Mäntysaari, B.Schenke, C. Shen and W. Zhao, Phys. Lett. B 833 (2022), 137348.

Proton geometry fluctuations

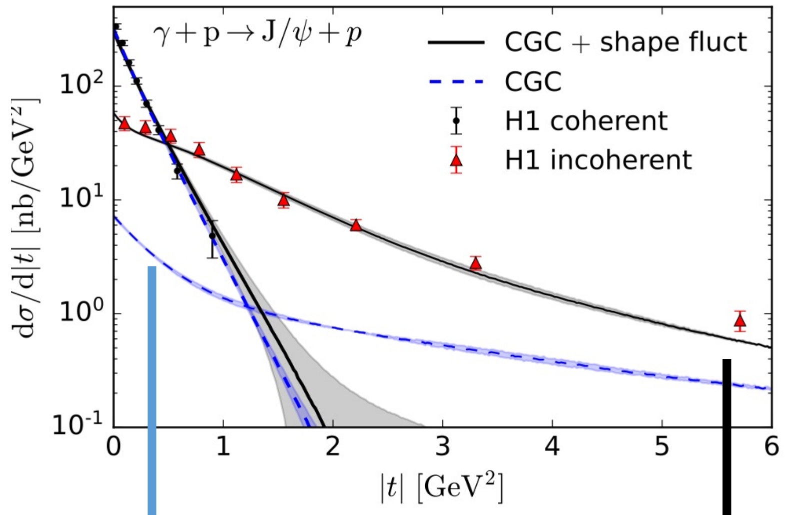

No subnucleon fluctuations

With subnucleon fluctuations

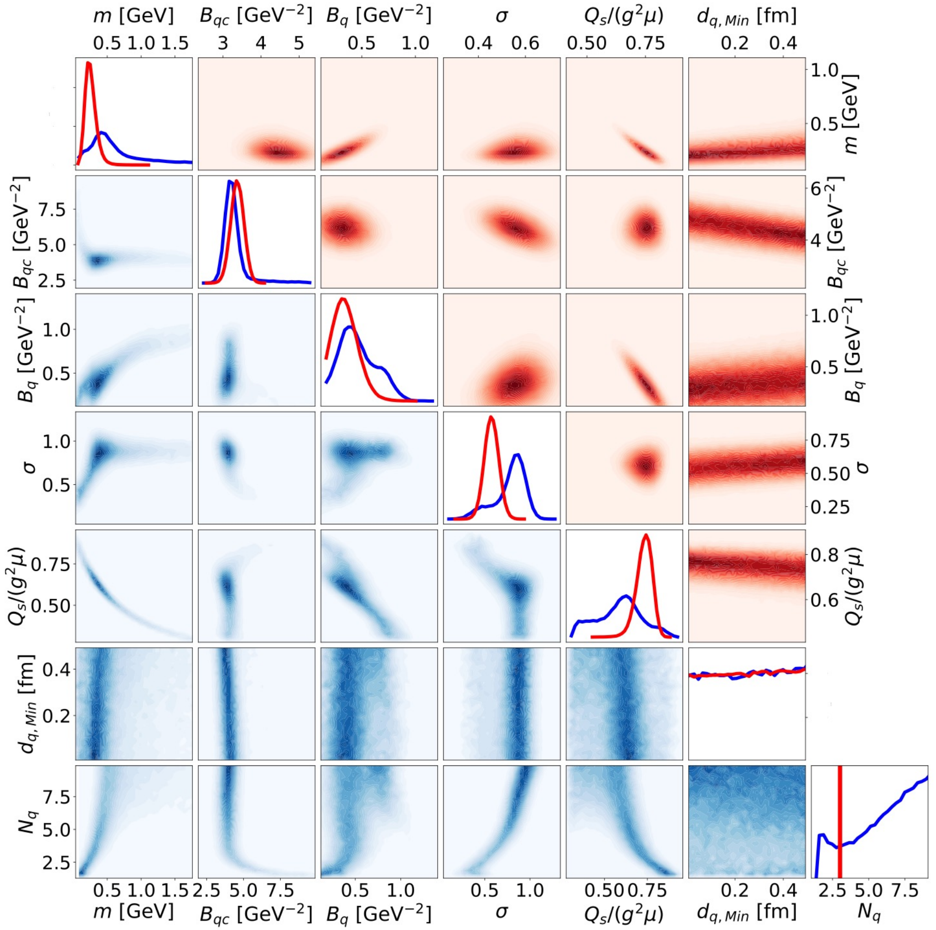

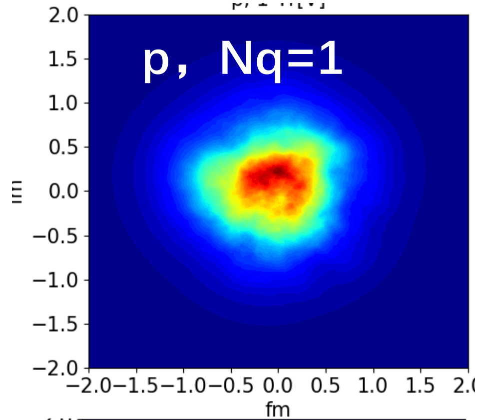

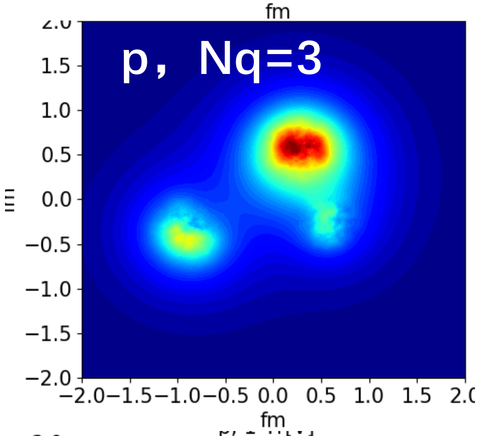

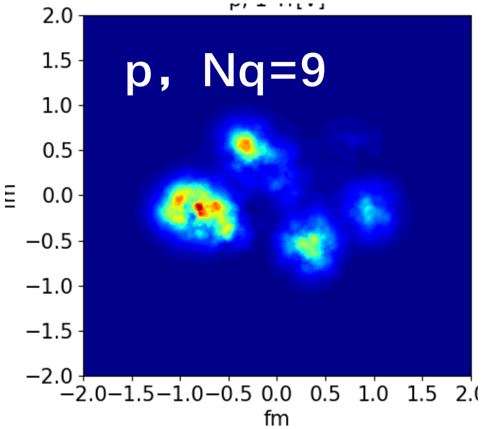

- Probe the event-by-event sub-nucleon fluctuations.
- Bayesian inference of the fluctuating proton shape.
- The extracted 2D RMS proton radius $R_{rms} = \sqrt{2(B_{qc} + B_q)}$ ~ **0.6 fm**.

H. Mäntysaari, Schenke , PhysRevLett.108.252301 , PhysRevC.86.034908 ;
H. Mäntysaari, F. Salazar and B. Schenke, Phys. Rev. D 106, 074019 (2022).
H. Mäntysaari, B.Schenke, C. Shen and W. Zhao, Phys. Lett. B 833 (2022), 137348.

Multi-scale imaging of Nuclear shape

$$\rho(r,\Theta,\Phi) \propto \frac{1}{1+\exp\left(\left[r-R(\Theta,\Phi)\right]/a\right)}\ ,\quad R(\Theta,\Phi)=R_0\left[1+\beta_2\left(\cos\gamma Y_{20}(\Theta)+\sin\gamma Y_{22}(\Theta,\Phi)\right)+\beta_3 Y_{30}(\Theta)+\beta_4 Y_{40}(\Theta)\right]$$

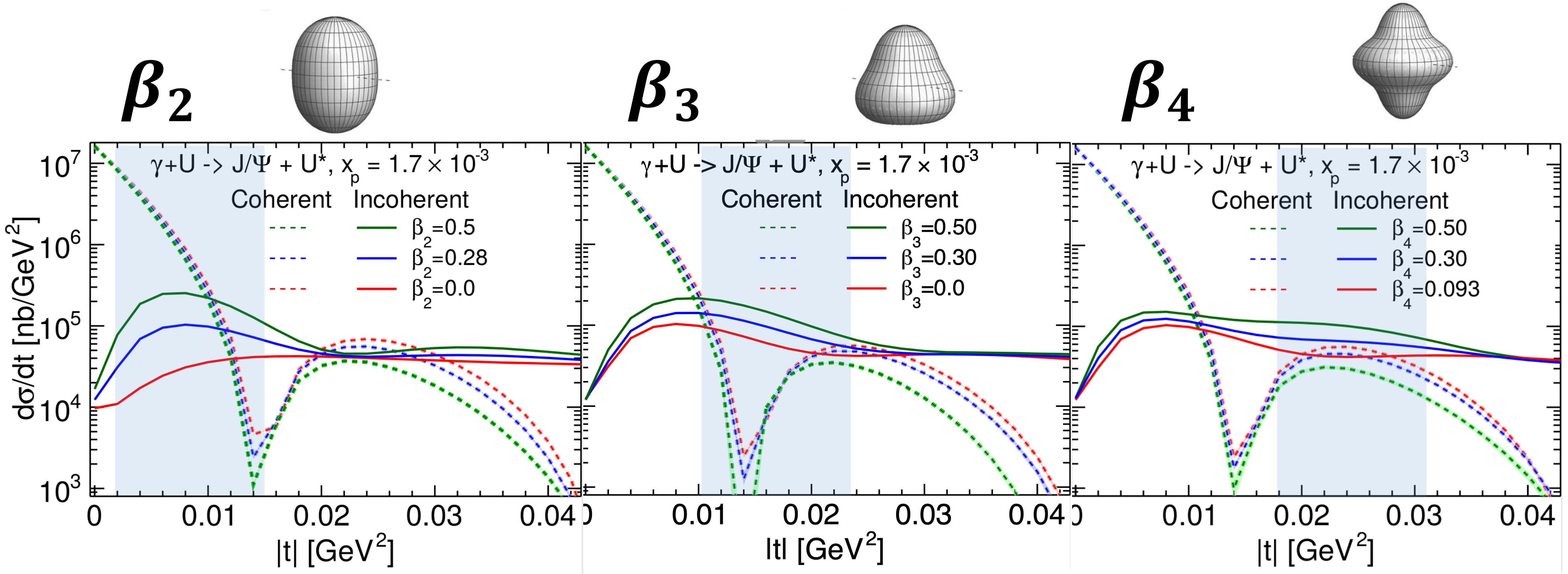

H. Mäntysaari, B.Schenke, C. Shen and W. Zhao, PhysRevLett.131.062301.

- It provides the "X-ray vision" for atoms.

Probing light nuclei structures

^{20}Ne

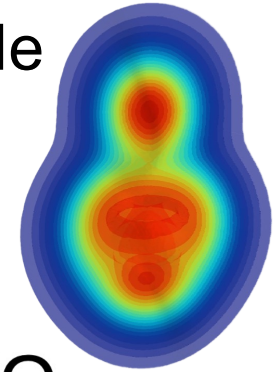

^{16}O

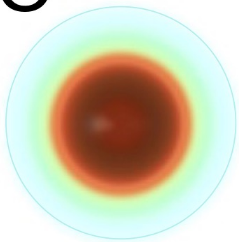

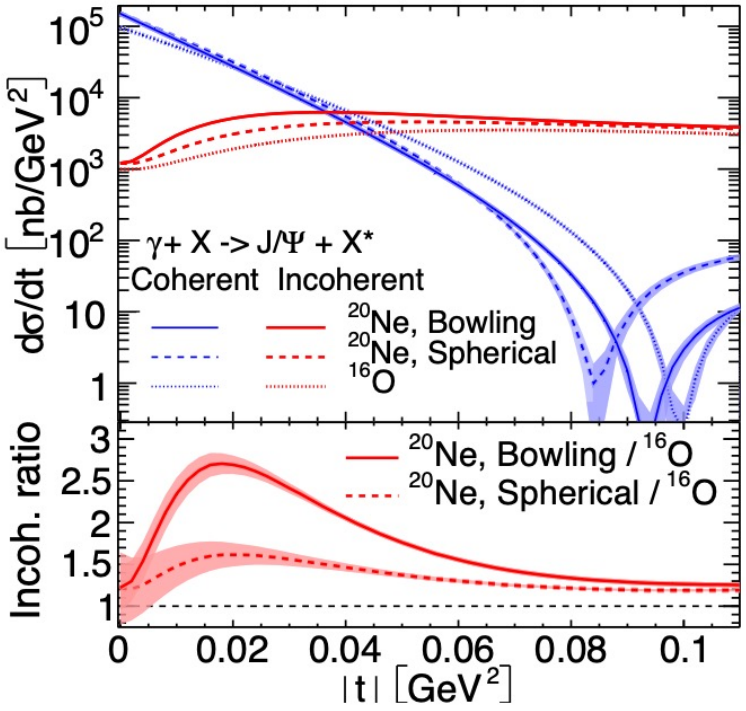

H. Mäntysaari, B.Schenke, C. Shen and W. Zhao, PRL.131.062301.

H. Mäntysaari, F. Salazar, B.Schenke, C. Shen and W. Zhao PRC.109.024908.

Probing light nuclei structures

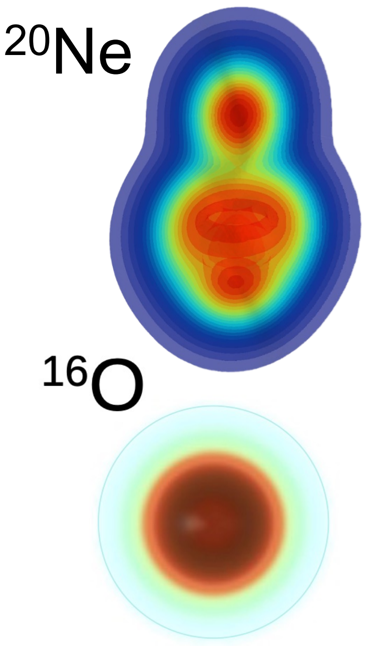

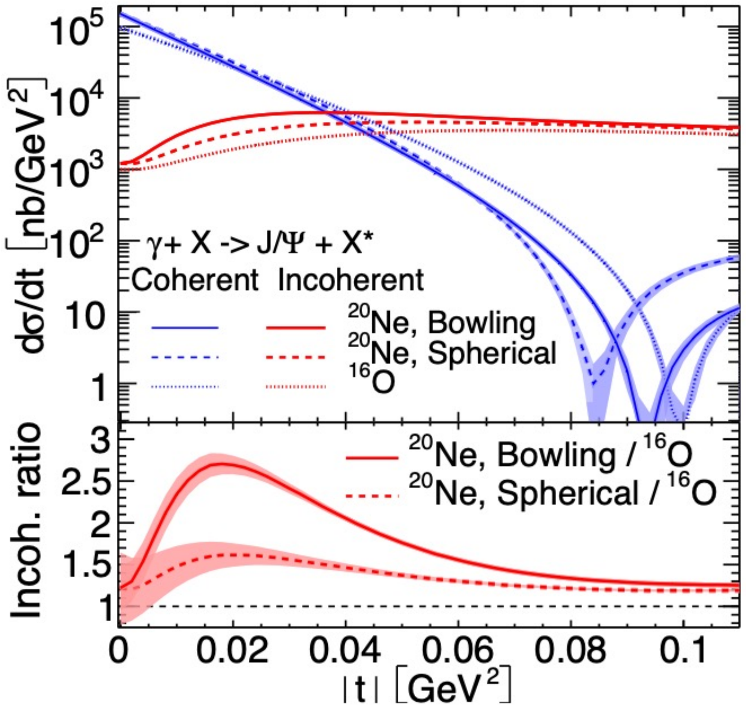

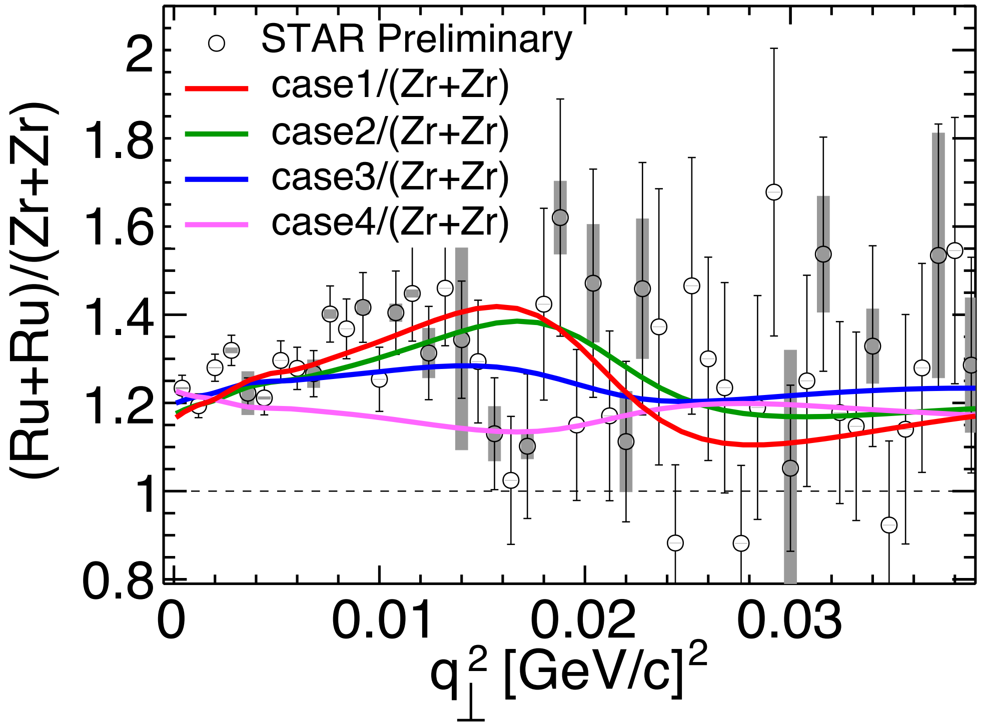

H. Mäntysaari, B.Schenke, C. Shen and W. Zhao, PRL.131.062301.
H. Mäntysaari, F. Salazar, B.Schenke, C. Shen and W. Zhao PRC.109.024908.

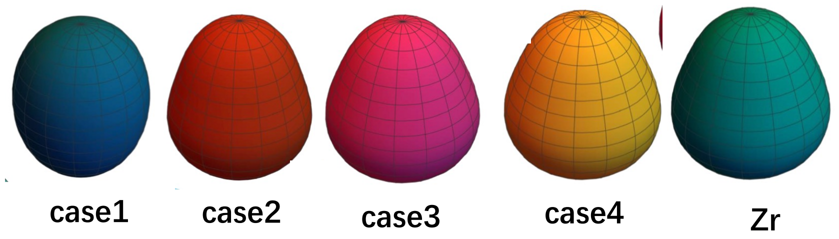

- Probe light nuclear structures by diffractive V.M. productions, complementary to heavy-ion observables. (See also J. P. Blaizot and G. Giacalone, [arXiv:2504.15421].)

Energy Evolution of Initial Conditions

Energy evolution of initial state

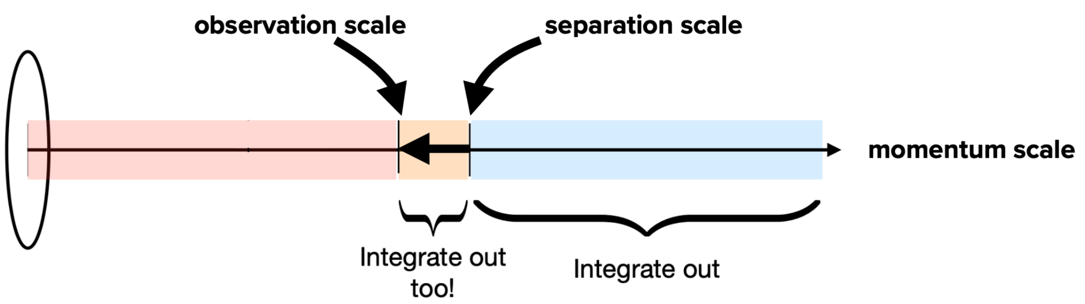

A. Morreale and F. Salazar, Universe 7, no.8, 312 (2021).

gluon density

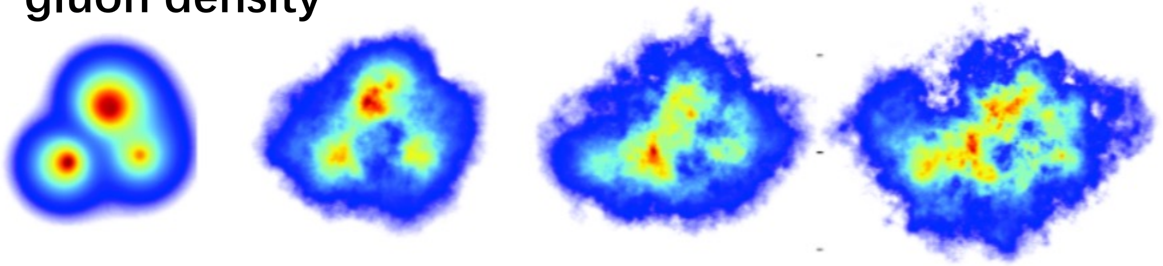

Low energy
(UPC/DIS)

High energy
(LHC)

- Energy evolution of the initial state.

H. Mäntysaari and B. Schenke, PRD 98 (2018) 034013.
H. Mäntysaari, B. Schenke, C, Shen and W. Zhao, PRL. 135, 022302 (2025)

Energy evolution of initial state

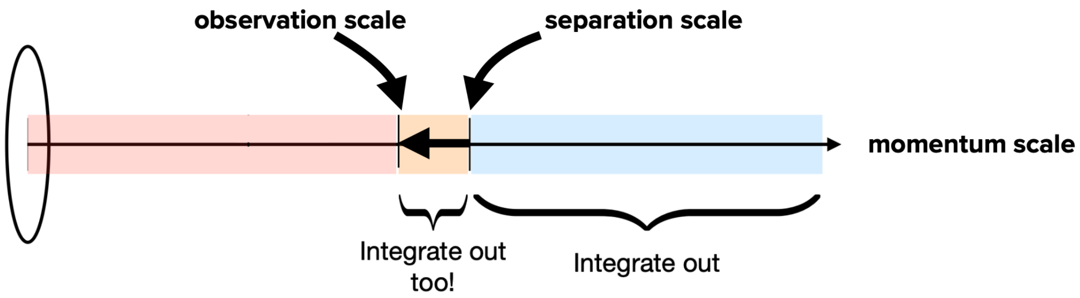

A. Morreale and F. Salazar, Universe 7, no.8, 312 (2021).

gluon density

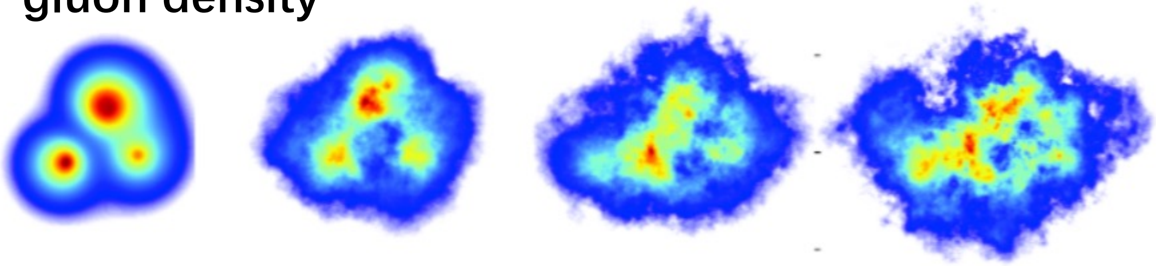

Low energy (UPC/DIS) → High energy (LHC)

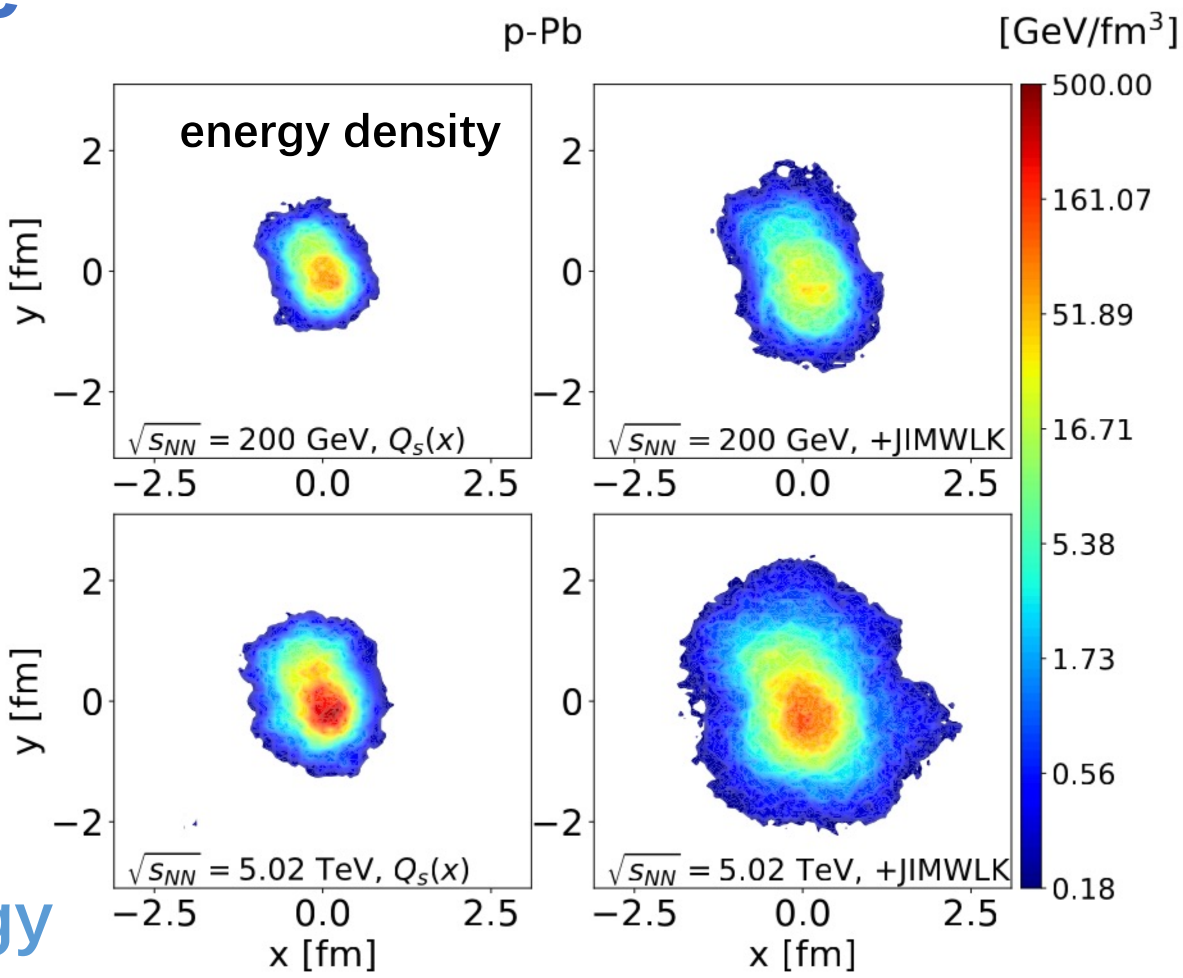

- Energy evolution of the initial state.

H. Mäntysaari and B. Schenke, PRD 98 (2018) 034013.
H. Mäntysaari, B. Schenke, C, Shen and W. Zhao, PRL. 135, 022302 (2025)

Effects of energy evolution on heavy-ion observables

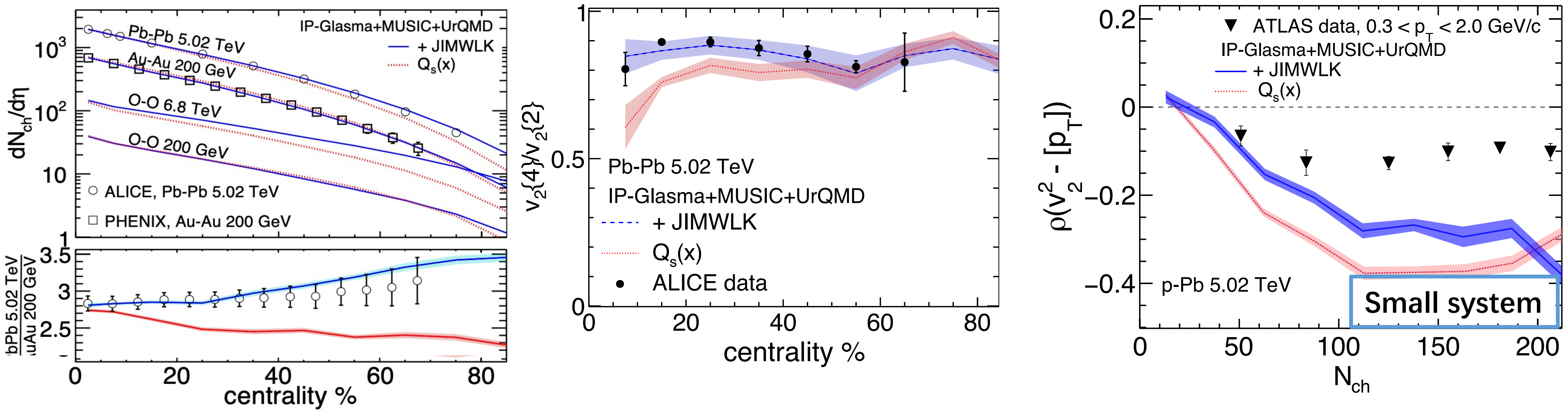

+ JIMWLK: CGC + energy evolution + Hydrodynamics

$\boldsymbol{Q_s(x)}$: CGC (change the $Q_s(x)$ only for different energies) + Hydrodynamics

H. Mäntysaari, B. Schenke, C, Shen and W. Zhao, PRL. 135, 022302 (2025)

- The energy evolution of the initial state is important in Bayesian analysis when comparing data across different collision energies.

Effects of energy evolution on heavy-ion observables

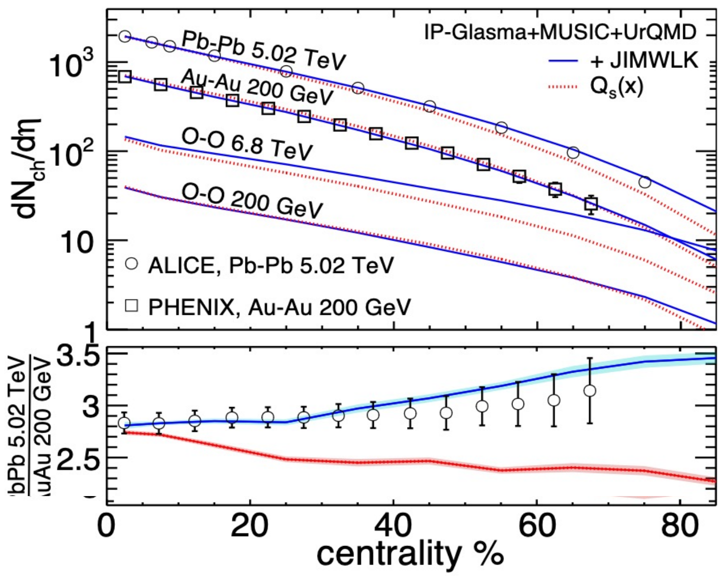

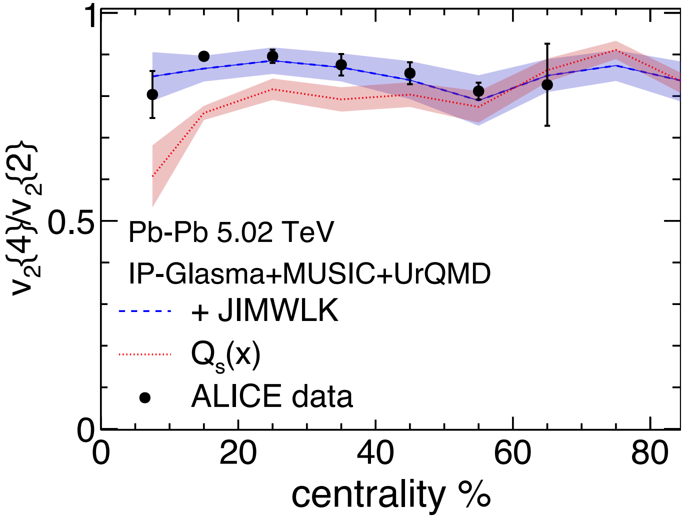

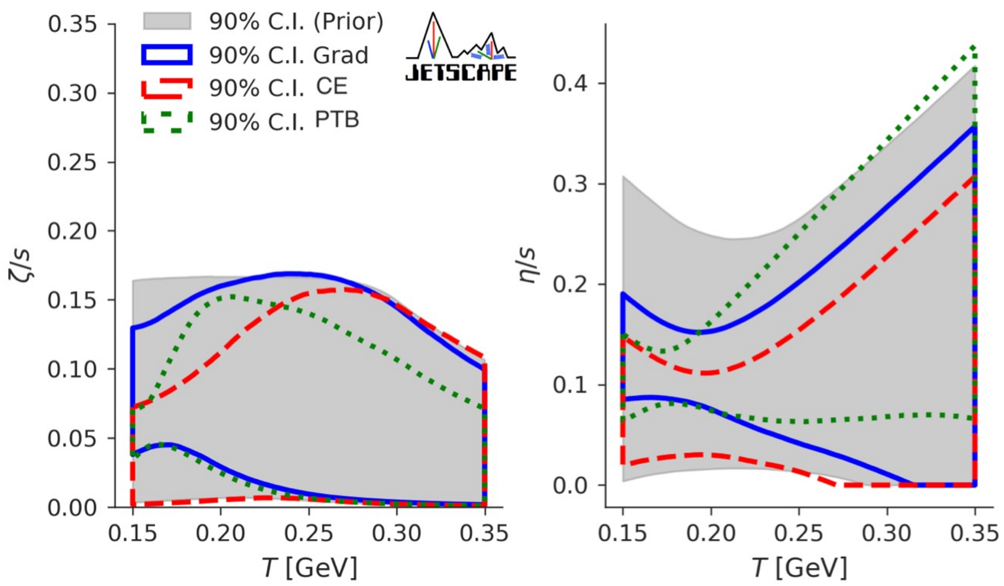

+ JIMWLK: CGC + energy evolution + Hydrodynamics

$\boldsymbol{Q_s(x)}$: CGC (change the $Q_s(x)$ only for different energies) + Hydrodynamics

JETSCAPE, PRC.103.054904

Bayesian fitting to the RHIC and LHC data.

H. Mäntysaari, B. Schenke, C, Shen and W. Zhao, PRL. 135, 022302 (2025)

- The energy evolution of the initial state is important in Bayesian analysis when comparing data across different collision energies.

Flow ratio NeNe/OO

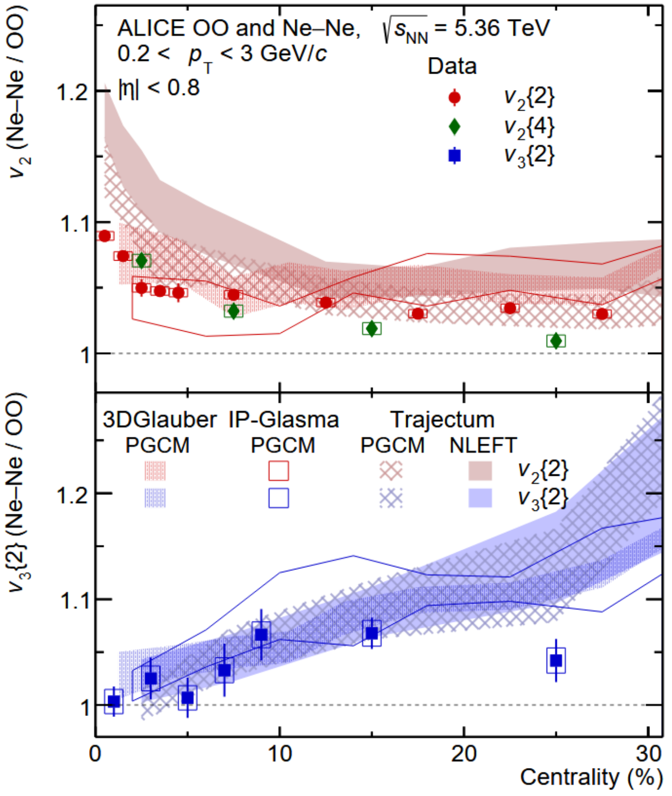

ALICE: [arXiv:2509.06428].

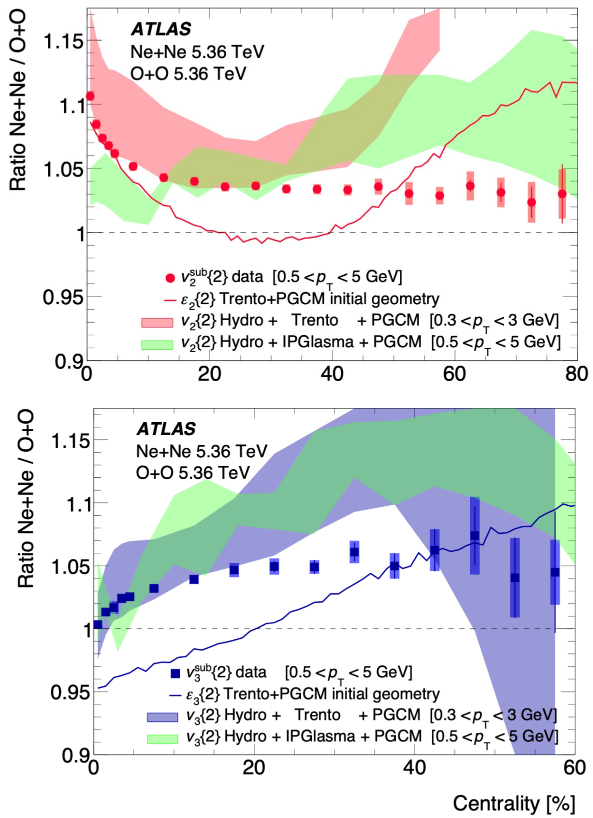

ATLAS: [arXiv:2509.05171].

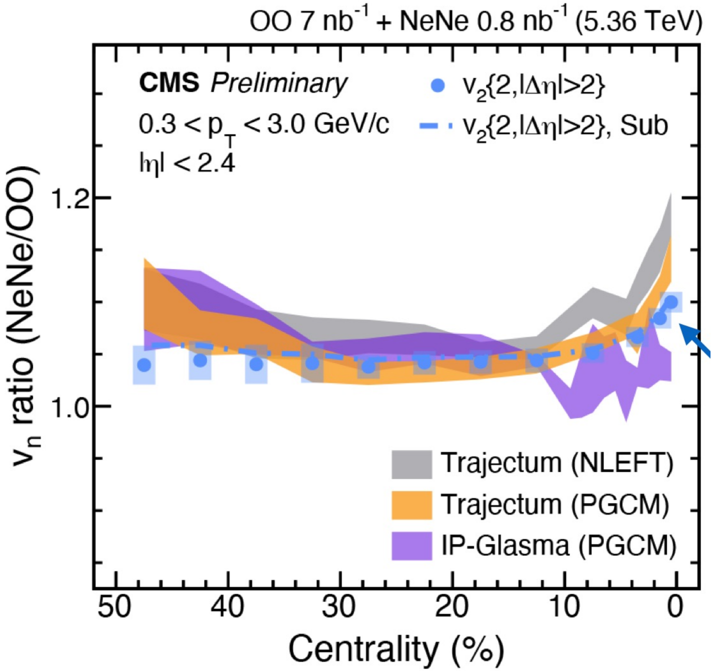

CMS: [arXiv:2510.02580].

- **Trajectum:** Fit Pb-Pb LHC flow data, [PRL,135, 012302]
- **IPGlasma + JIMWLK:** Fit J/Ψ data + energy evolution [PRL, 135,022302]
- **3DGlauber:** Fit dAu, AuAu at RHIC, then extrapolate to LHC. [JETSCAPE, in preparation]

Playing Relativistic Bowling Ball

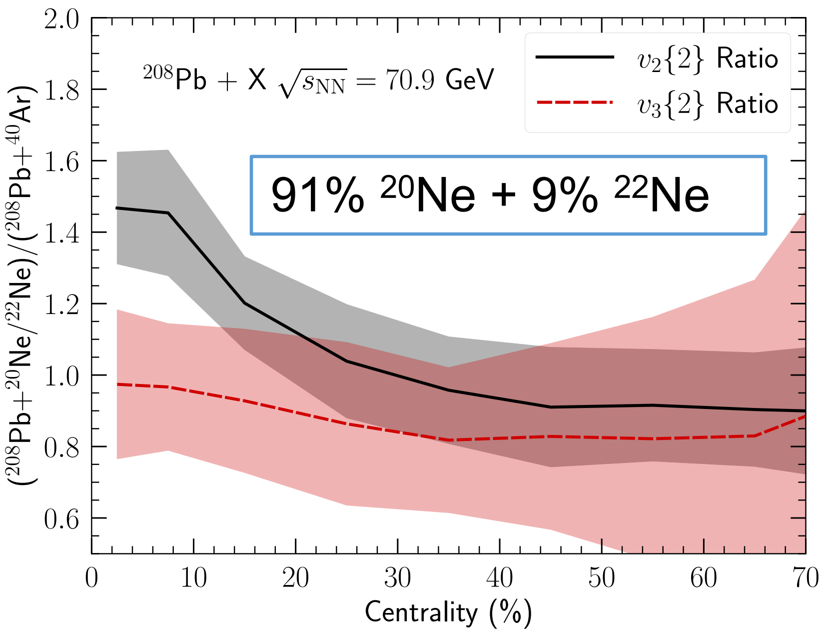

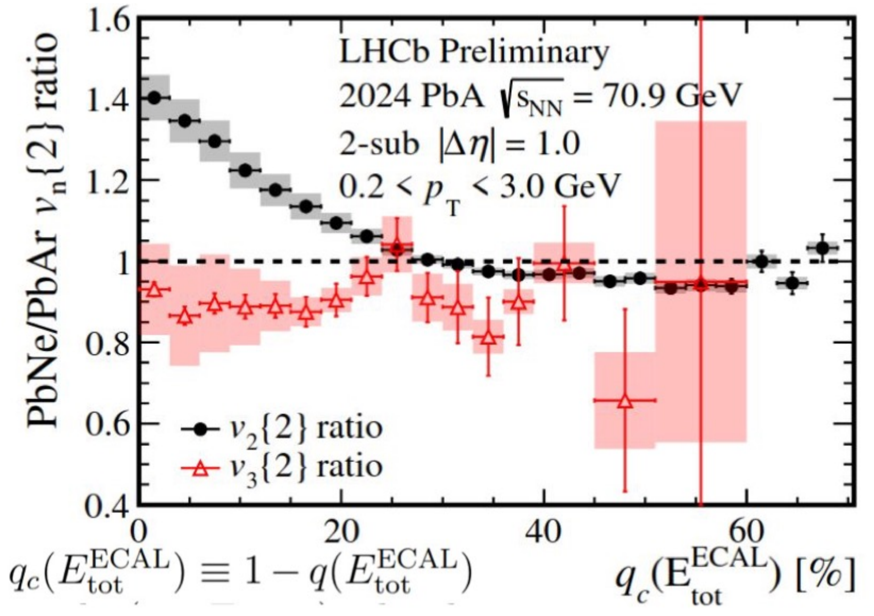

(Generated by ChatGPT)

LHCb: [arXiv:2509.12399].

Playing Relativistic Bowling Ball

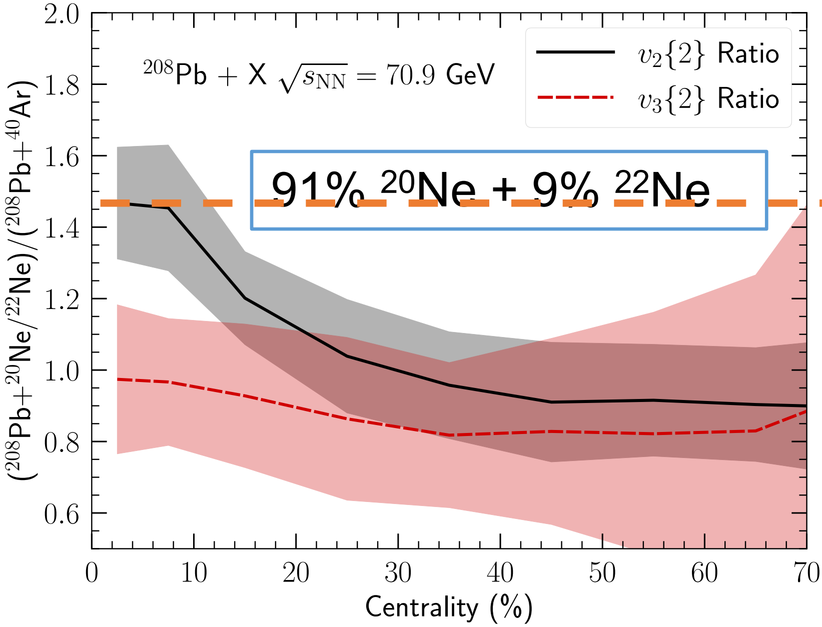

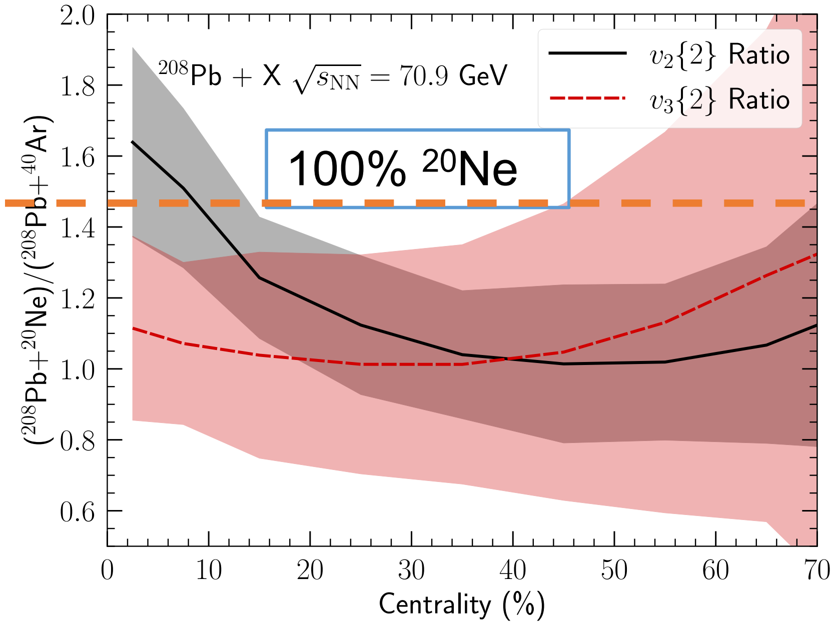

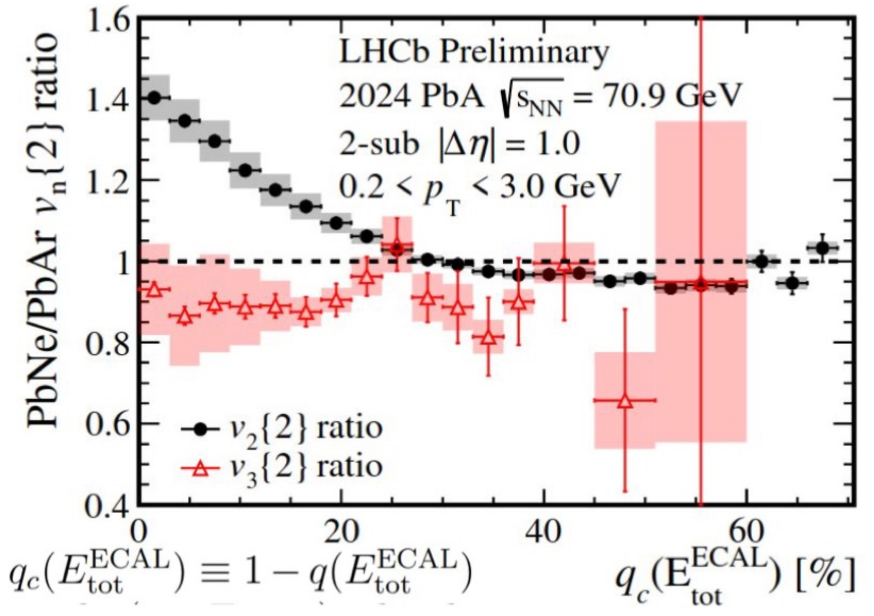

- Mixing 9% of ^{22}Ne has a sizable effect on the v_n ratio.

LHCb: [arXiv:2509.12399].

Probing gluon saturations in UPC

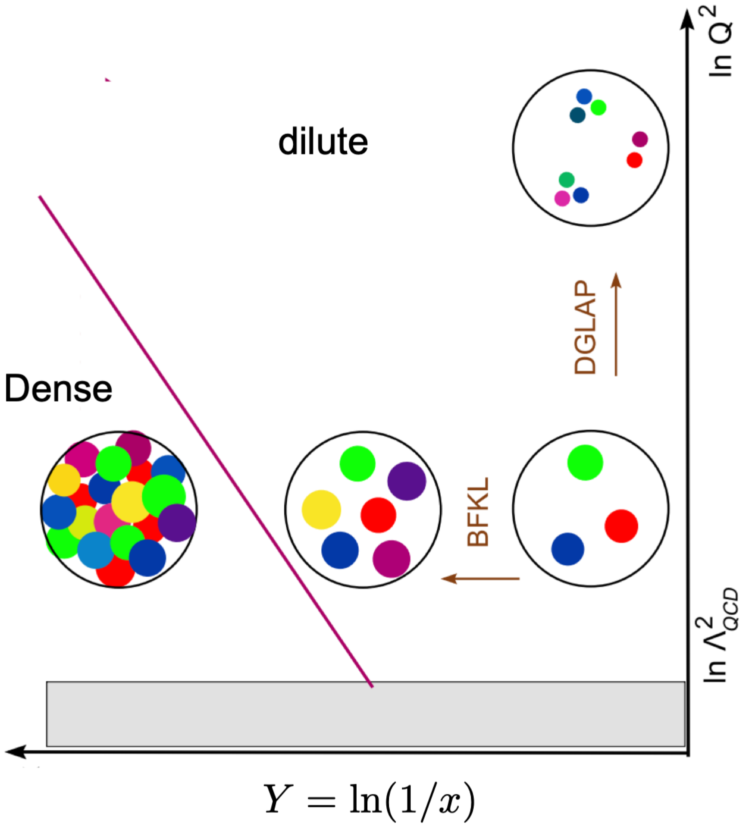

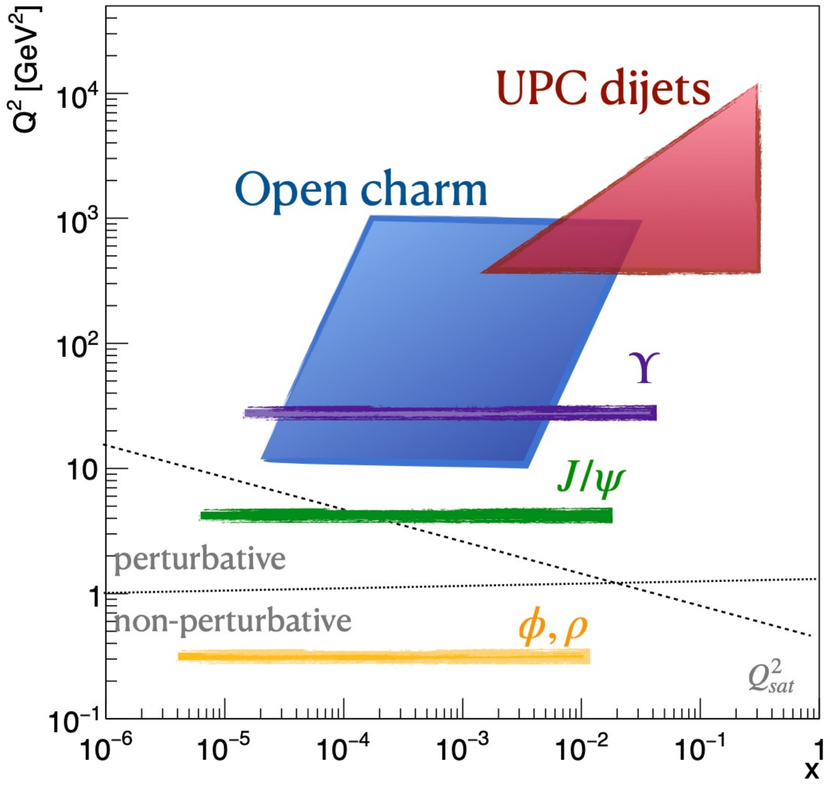

Wealth of vector meson productions in UPCs

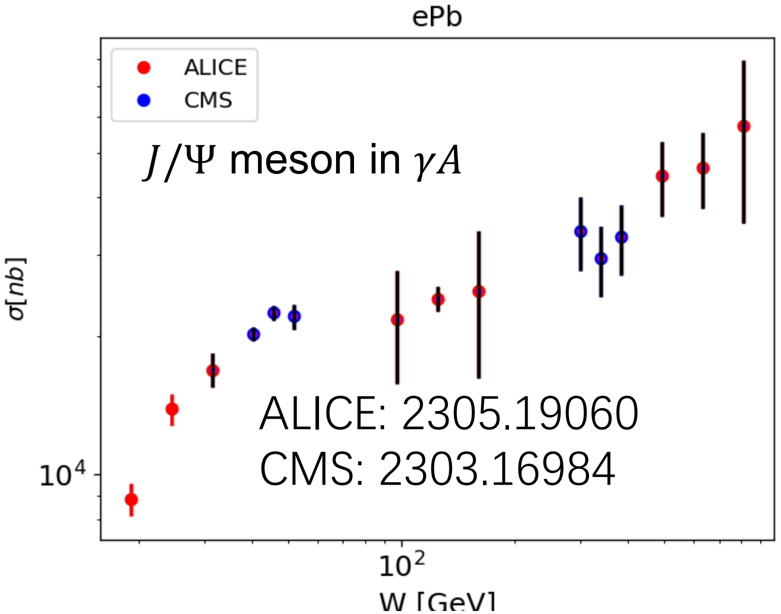

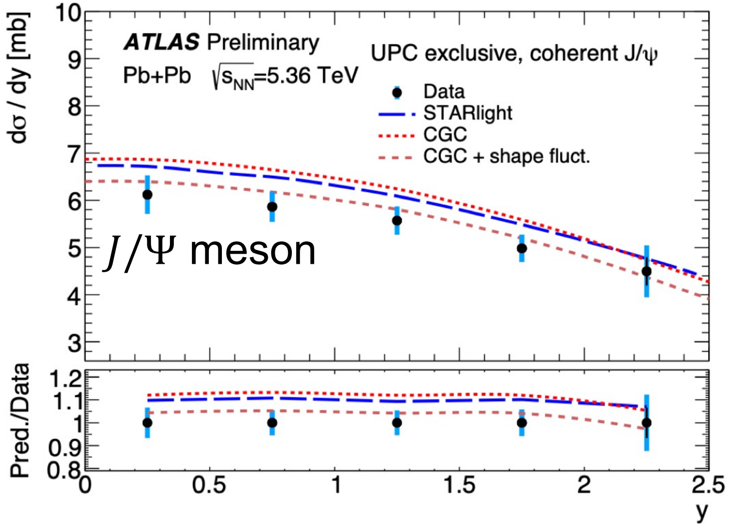

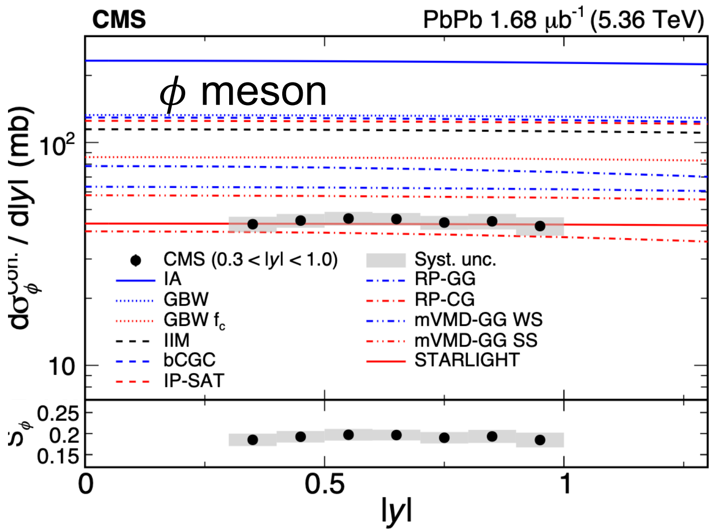

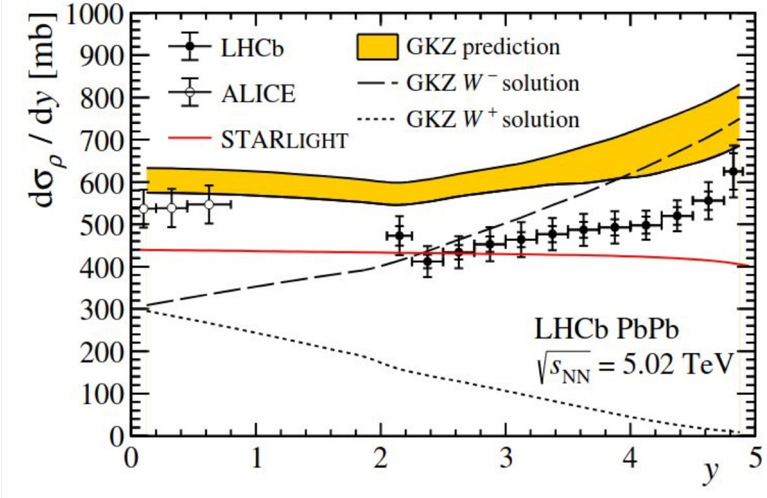

- Incoherent γA energy dependence at different | t |

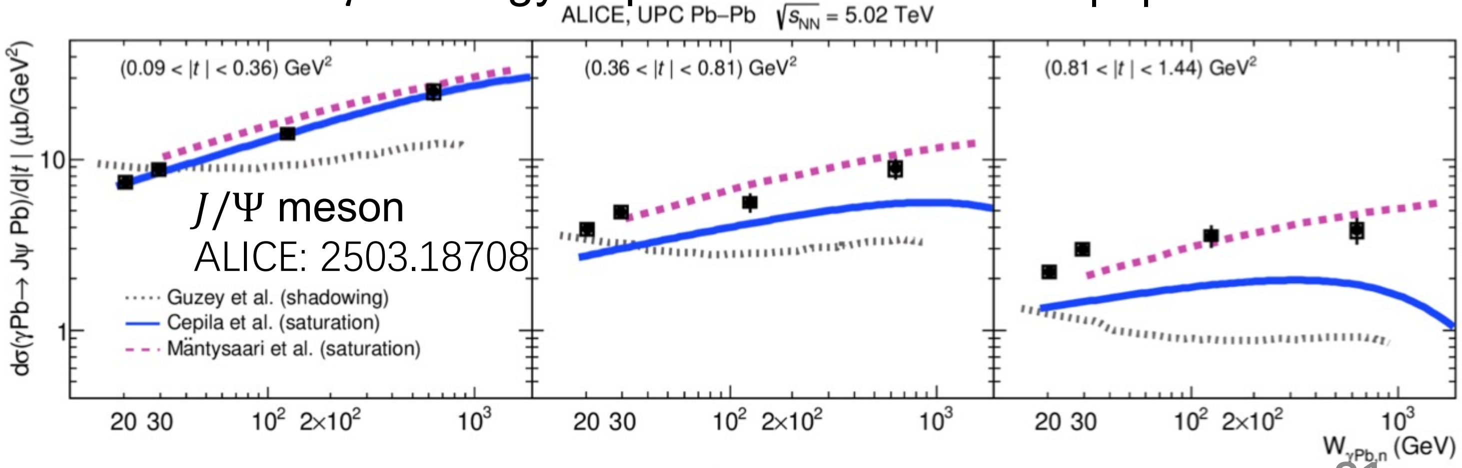

Model calculations

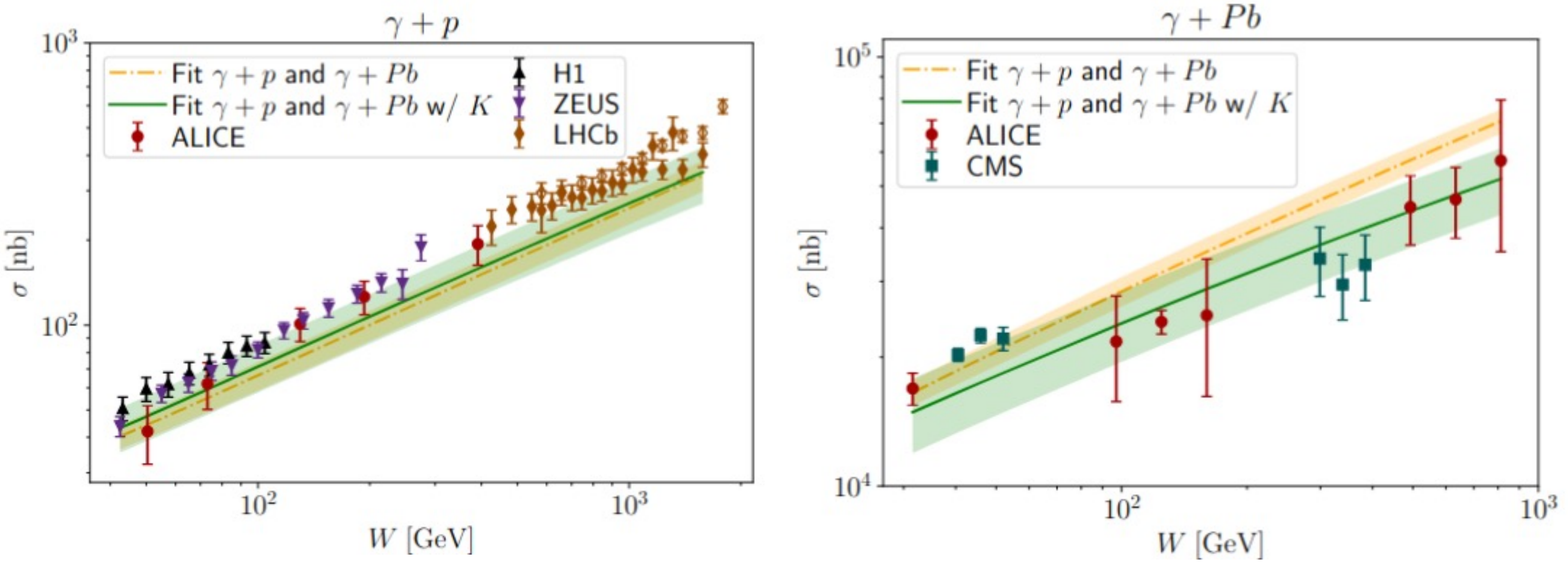

H. Mantysaari, etc, al., arXiv:2507.14087.

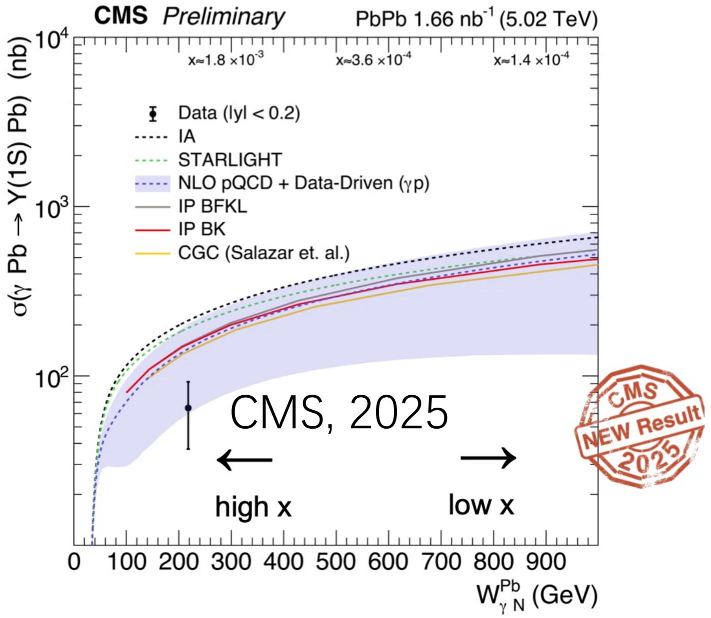

- CGC model has **tension** to fit the γp and γPb data simultaneously. (See also: J. Penttala and C. Royon, PLB. 864, 139394 (2025).)
- Preliminary CMS data shows **more suppression** for $\Upsilon(1s)$ than CGC predictions.

Dihadron Angular Correlations in Forward pp and pA collisions

Forward di-hadrons productions (dilute-dense)

- large-x projectile (proton) on small-x target (proton or nucleus)

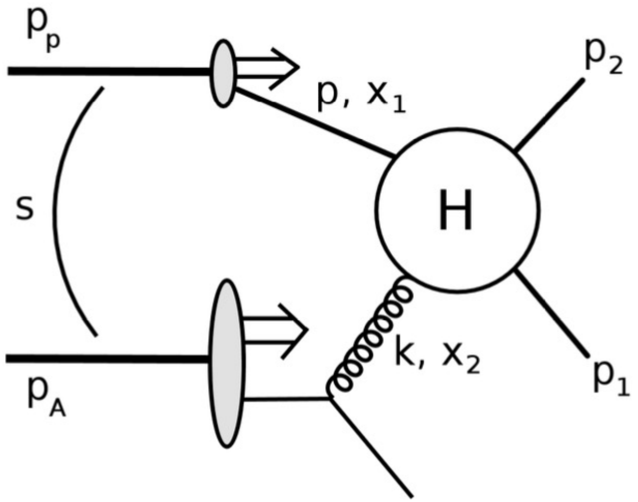

$\langle k_{1t} \rangle \sim \Lambda_{QCD}$ $\langle k_{2t} \rangle \sim Q_s(x_2)$

$Q_s(x_2) \gg \Lambda_{QCD}$

so-called "dilute-dense" kinematics

Incoming partons' energy fractions:

$$x_1 = \frac{1}{\sqrt{s}}\left(|p_{1t}|e^{y_1} + |p_{2t}|e^{y_2}\right) \qquad \xrightarrow{y_1, y_2 \gg 0} \qquad x_1 \sim 1$$

$$x_2 = \frac{1}{\sqrt{s}}\left(|p_{1t}|e^{-y_1} + |p_{2t}|e^{-y_2}\right) \qquad\qquad\qquad x_2 \ll 1$$

CM (2007)

Gluon's transverse momentum (p_{1t}, p_{2t} imbalance):

$$|k_t|^2 = |p_{1t} + p_{2t}|^2 = |p_{1t}|^2 + |p_{2t}|^2 + 2|p_{1t}||p_{2t}|\cos\Delta\phi$$

prediction: modification of the k_t distribution in p+Pb vs p+p collisions

Borrow from Cyrille Marquet's (2020) slide

STAR measurements

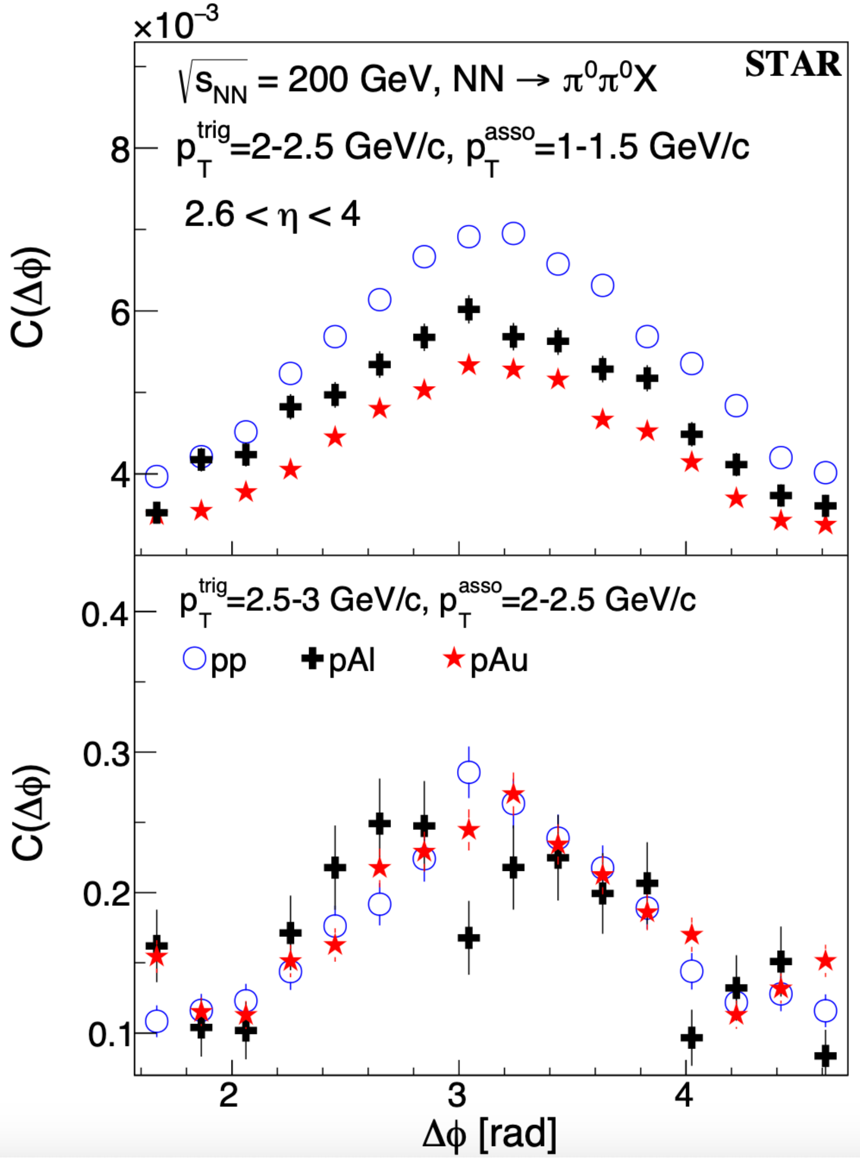

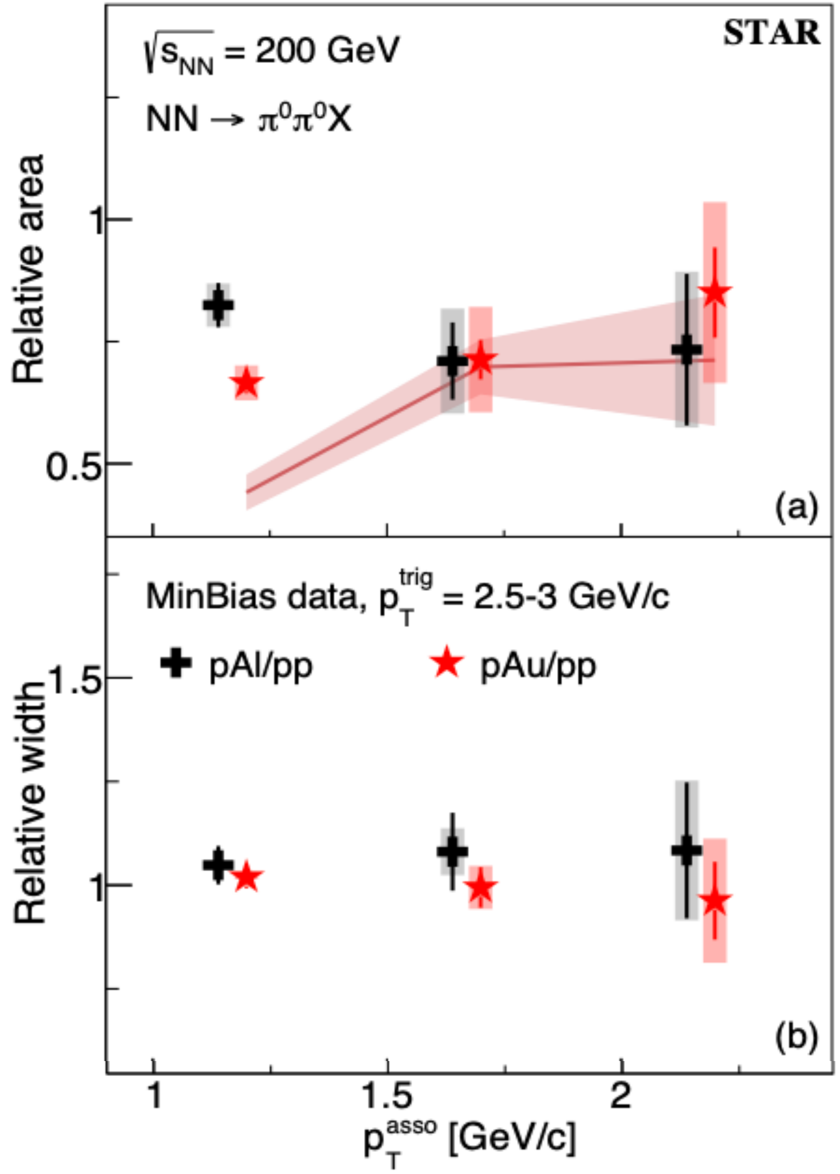

STAR data: PhysRevLett.129.092501.

CGC model: J. L. Albacete, G. Giacalone, C. Marquet and M. Matas, PhysRevD.99.014002

Color Glass Condensate Calculations

- We use the (massless) improved TMD factorization (ITMD), which resums the $\left(\frac{Q_s}{k_T}\right)^n$ and $\left(\frac{k_T}{P_T}\right)^n$.

$$\frac{d\sigma^{pA\to \text{dijets}+X}}{dy_1 dy_2 d^2p_{1t} d^2p_{2t}} = \frac{\alpha_s^2}{(x_1x_2s)^2} \sum_{a,c,d} x_1 f_{a/p}(x_1,\mu^2) \sum_i H^{(i)}_{ag\to cd} \mathcal{F}^{(i)}_{ag}(x_2,k_t) \frac{1}{1+\delta_{cd}},$$

$f_{a/p}$: Collinear pdf for the large-x projectile (dilute part)

$F^i_{ag}(x,k_t)$: Several gluon TMDs for small-x target (dense part)

$H^i_{ag\to cd}$: The associated hard matrix elements.

Cyrille Marquet's slide (2020);
P. Kotko, K. Kutak, C. Marquet, E. Petreska, S. Sapeta and A. van Hameren, JHEP09(2015)106

Soft gluon resummation and TMDs

A. H. Mueller, B. W. Xiao and F. Yuan, PhysRevLett.110.082301.

- Sudakov factors for soft gluon resummation :

$$\frac{d\sigma}{d^2p_{T1}d^2p_{T2}} \propto \int \frac{d^2b_\perp}{(2\pi)^2} e^{-i\vec{q}_T\cdot\vec{b}_\perp} f(x_1) \otimes F(x_2, b_\perp) \otimes H \otimes e^{-S_{\rm Sudakov}}$$

Soft gluon resummation and TMDs

A. H. Mueller, B. W. Xiao and F. Yuan, PhysRevLett.110.082301.

- Sudakov factors for soft gluon resummation :

$$\frac{d\sigma}{d^2p_{T1}d^2p_{T2}} \propto \int \frac{d^2b_\perp}{(2\pi)^2} e^{-i\vec{q}_T\cdot\vec{b}_\perp} f(x_1) \otimes F(x_2, b_\perp) \otimes H \otimes e^{-S_{\text{Sudakov}}}$$

- TMDs:

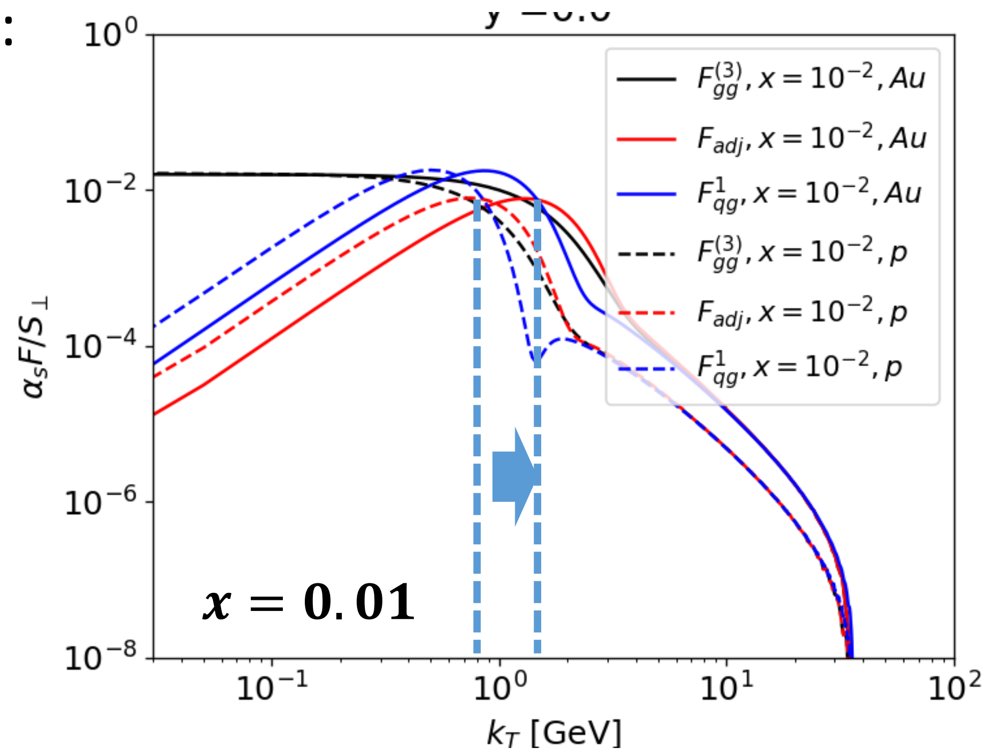

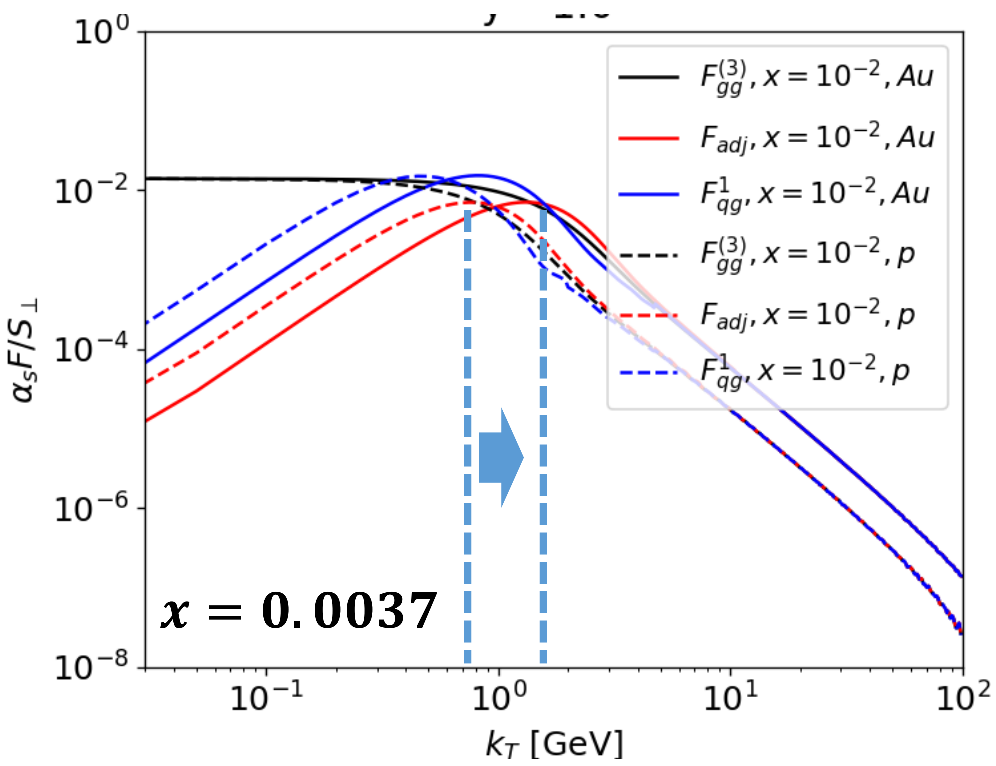

Dihadron Correlations in Forward pp and pA collisions

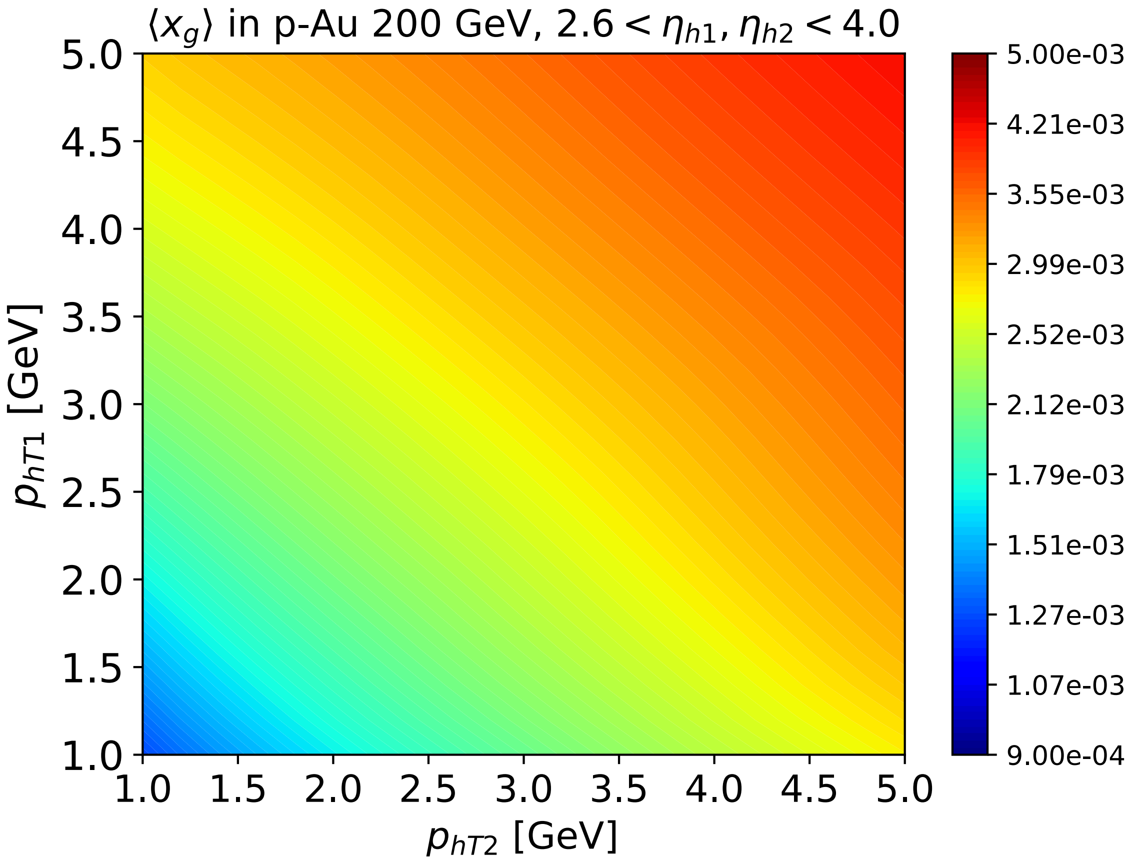

W. Zhao, etc. al. in progress.
STAR data: PhysRevLett.129.092501

- $< x_g >$ probed by di-hadron at STAR is small.

Dihadron Correlations in Forward pp and pA collisions

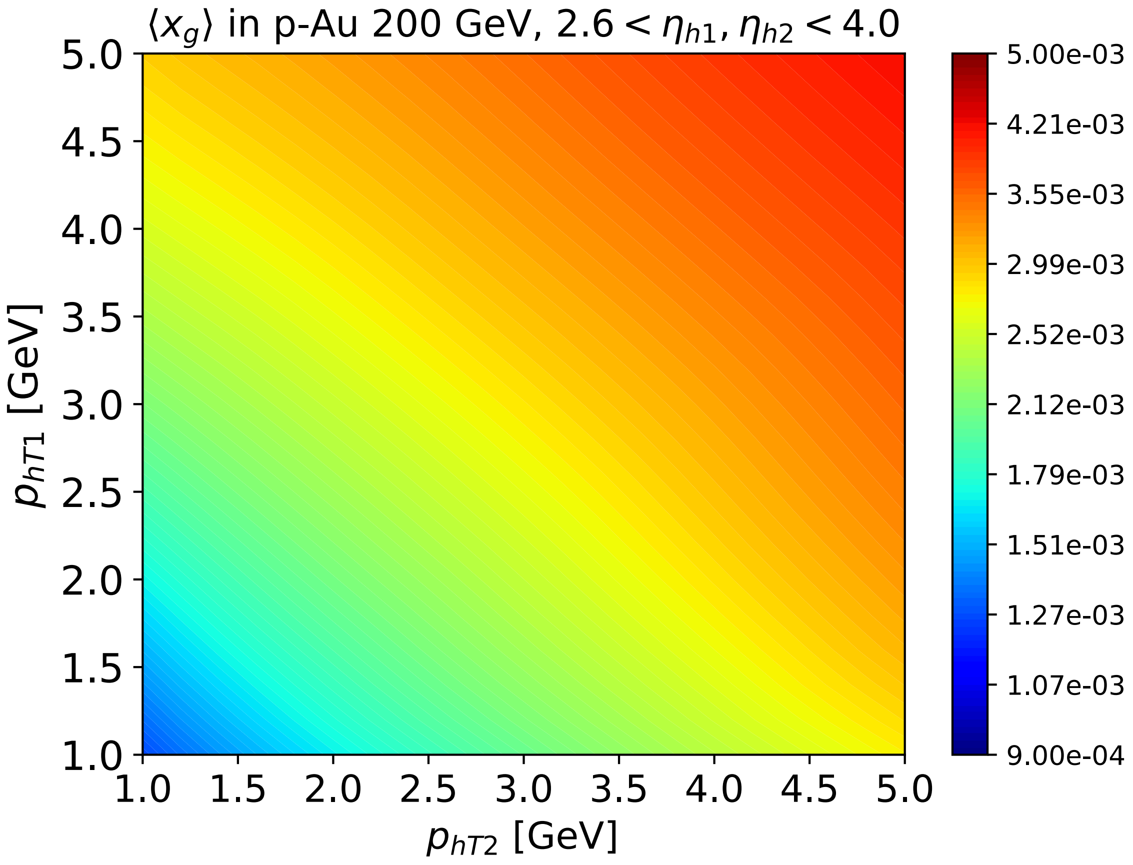

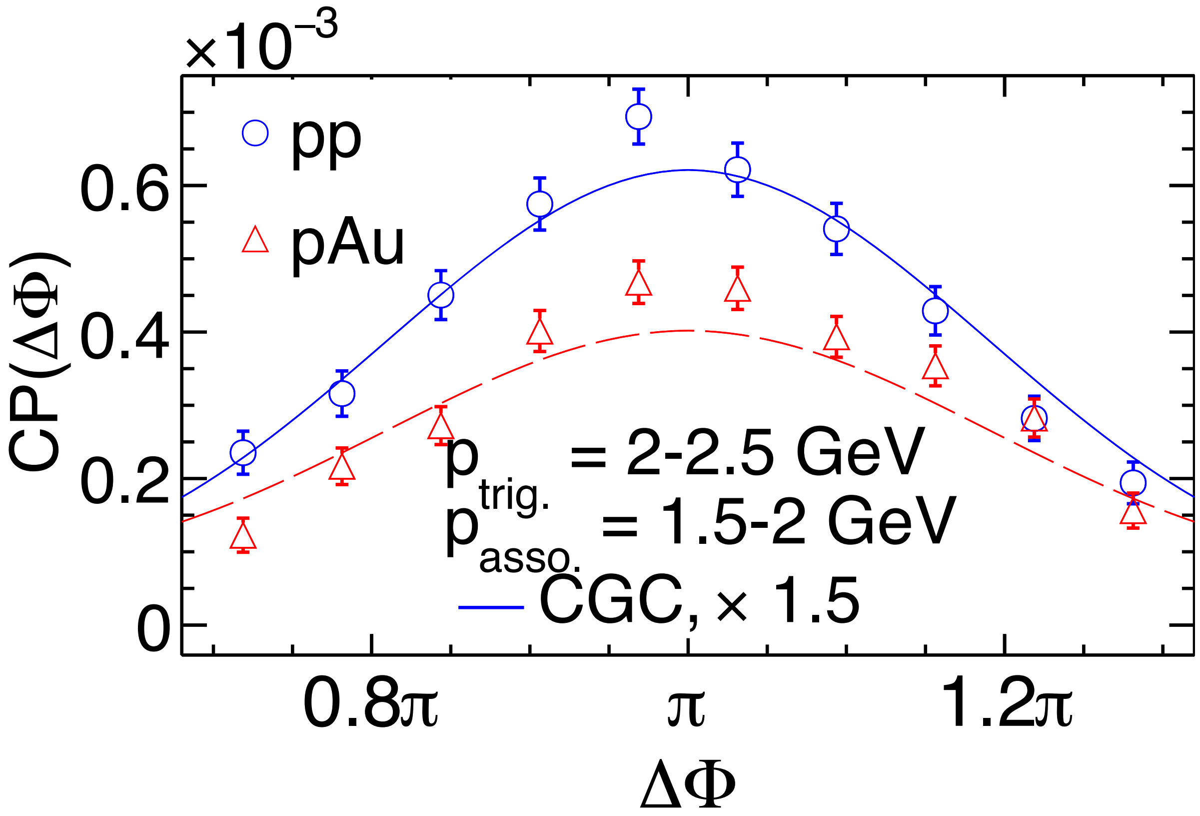

W. Zhao, etc. al. in progress.
STAR data: PhysRevLett.129.092501

- $< x_g >$ probed by di-hadron at STAR is small.
- CGC model reasonably describe the STAR data; Suppression: **pp > pAu.**

Dihadron Correlations in Forward collisions

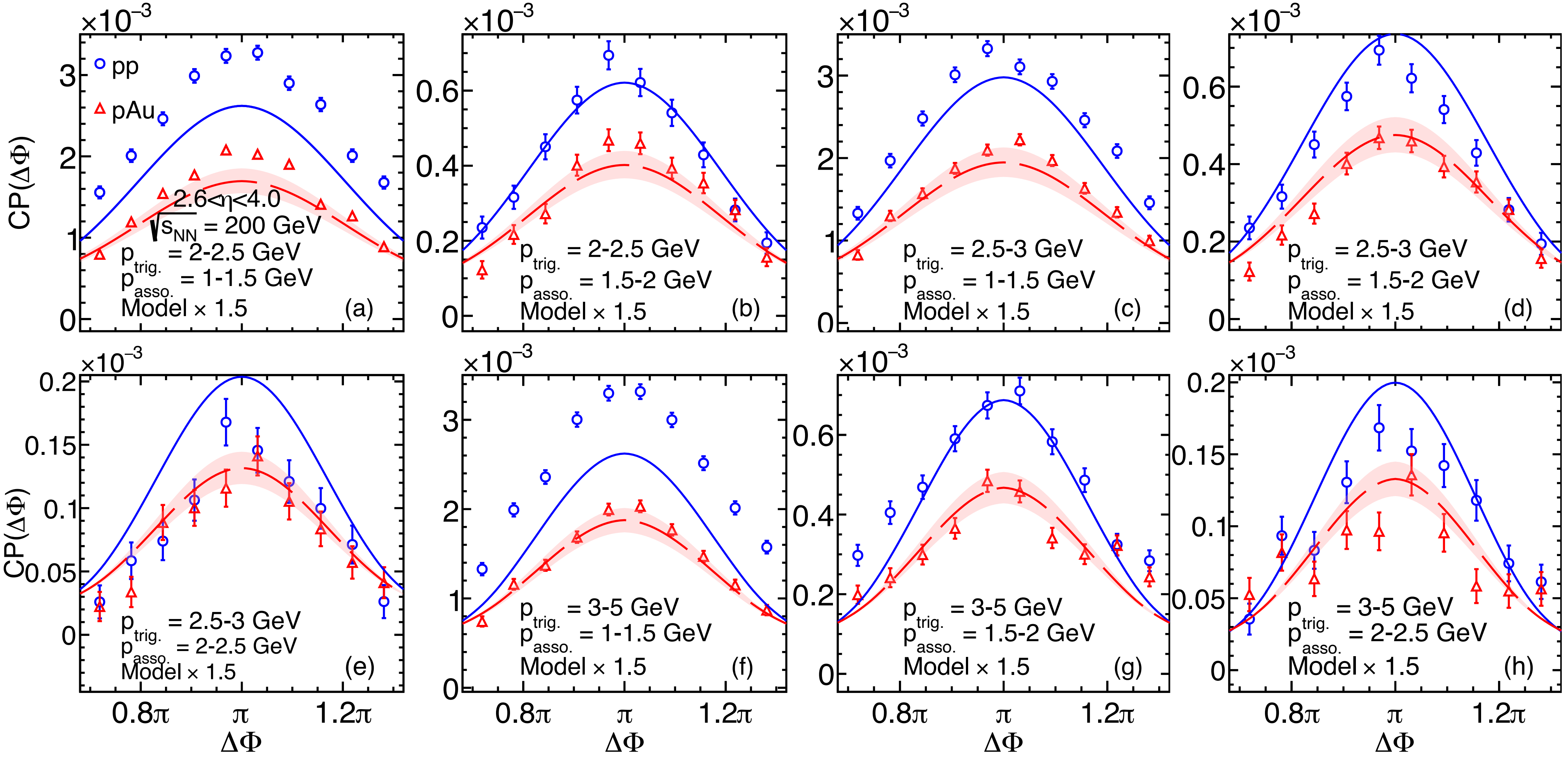

W. Zhao, etc. al. in progress.
STAR data: PhysRevLett.129.092501

- Overall, it's good; **Most asymmetric bins** not so good.
- Need an **additional normalization factor**. (There are uncertainties from FF).

Area ratio and width ratio between pAu and pp

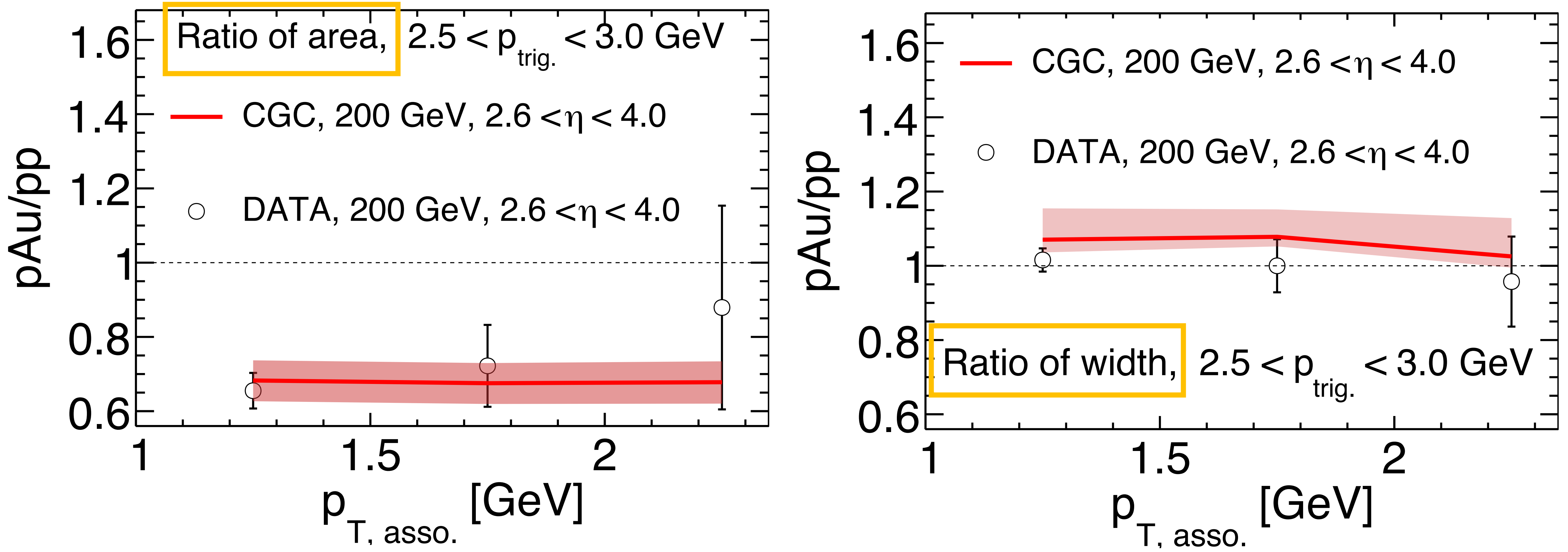

- CGC predicts **very week p_T dependence** at RHIC energy.

Predictions for LHCb at the LHC

p-p and p–Pb at $\sqrt{s_{nn}} = 8.16\ TeV, 2 < \eta < 5$

$< x_g >$ probed by STAR and LHCb

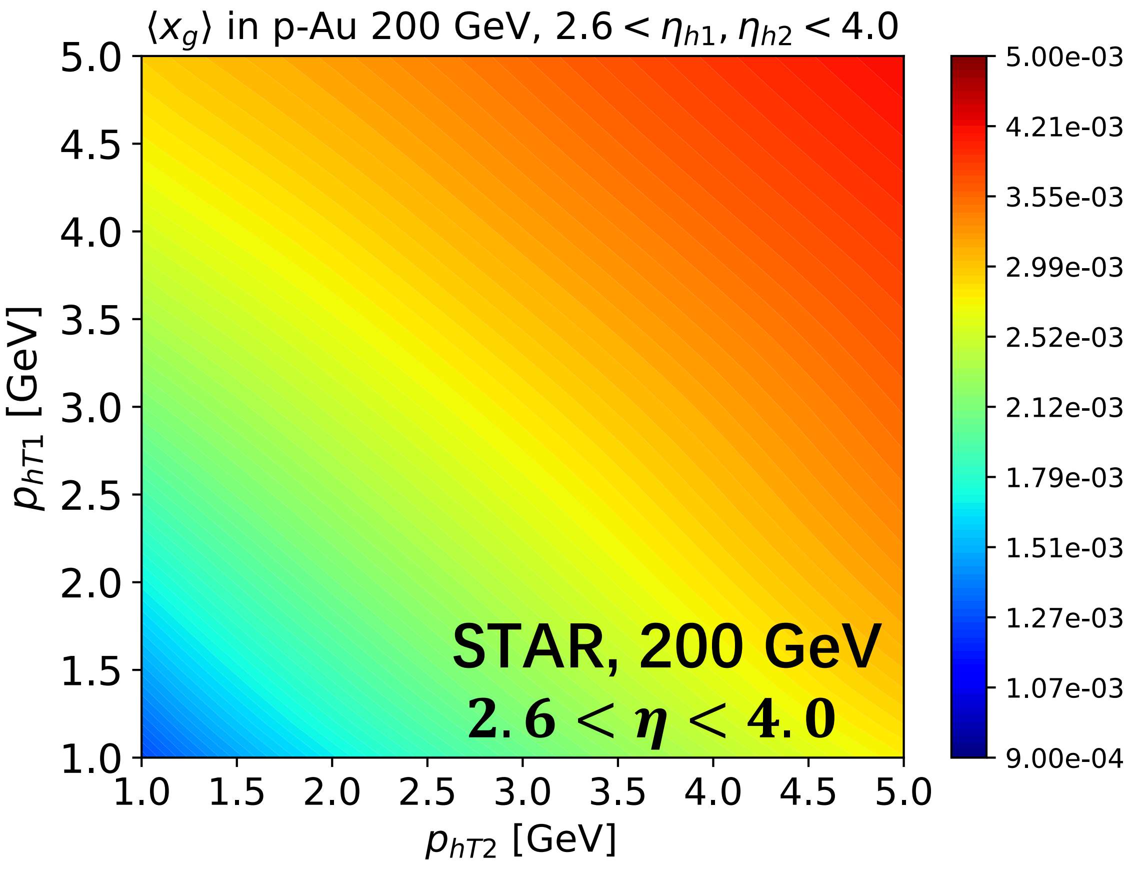

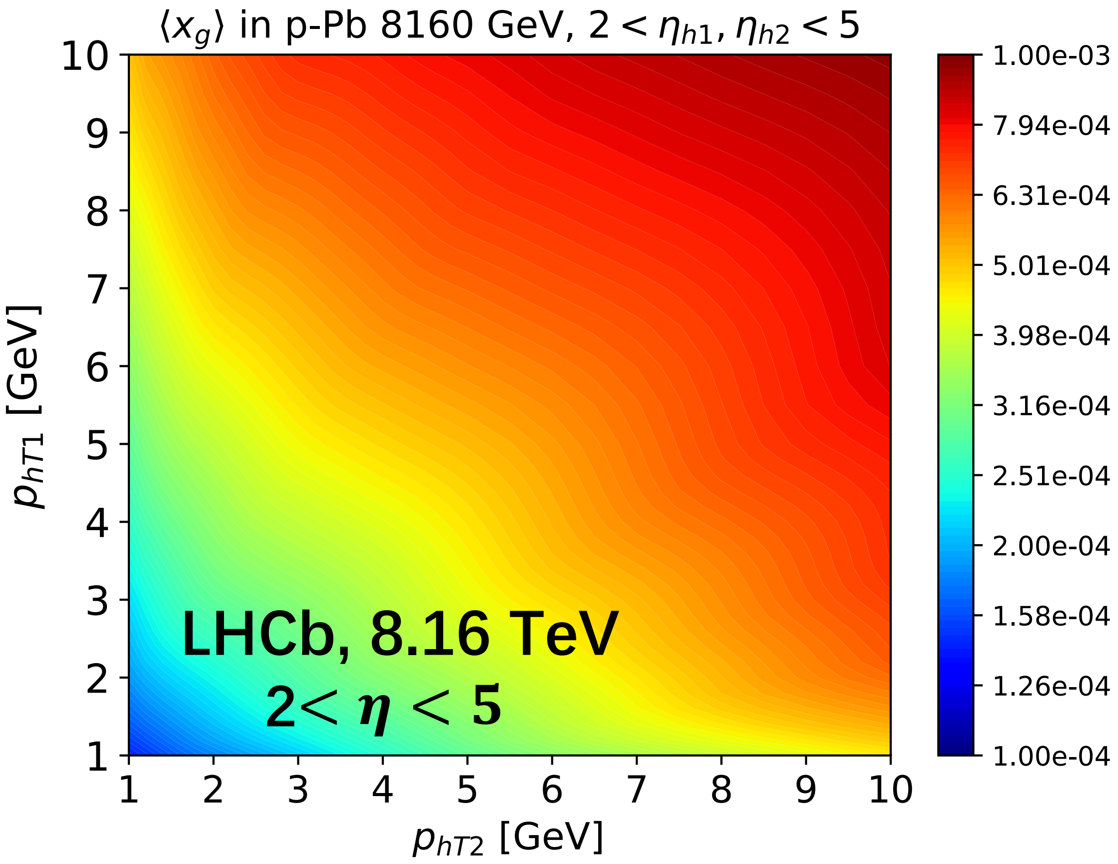

- $< x_g >$ probed by di-hadron at LHCb is **much smaller** than that at STAR.

Dihadron Correlations in LHCb

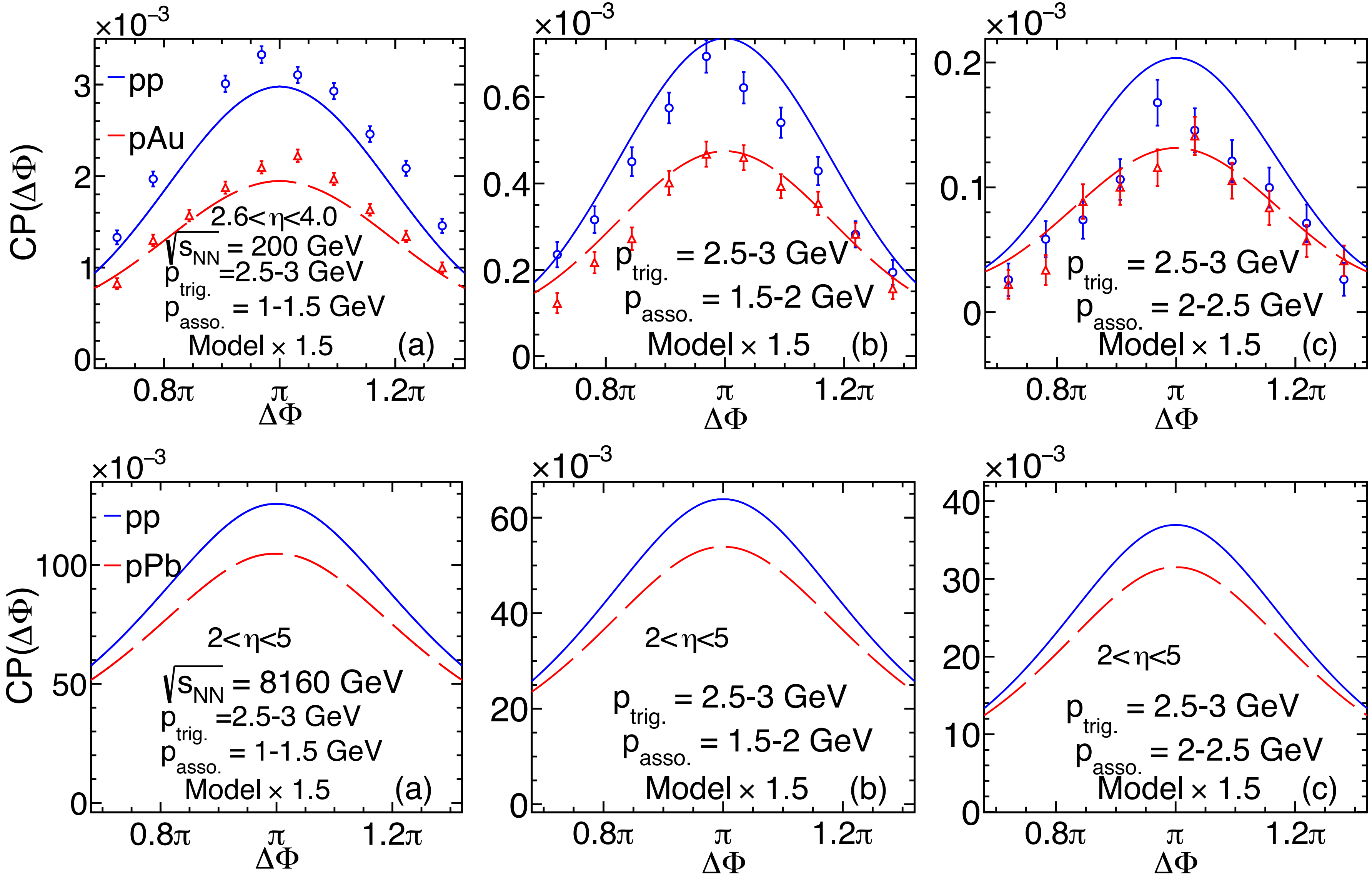

STAR, 200 GeV
$2.6 < \eta < 4.0$

LHCb, 8.16 TeV
$2 < \eta < 5$

- Surprisingly, LHCb has the **smaller suppression** than STAR, even LHCb has smaller x_g .

Dihadron Correlations in LHCb

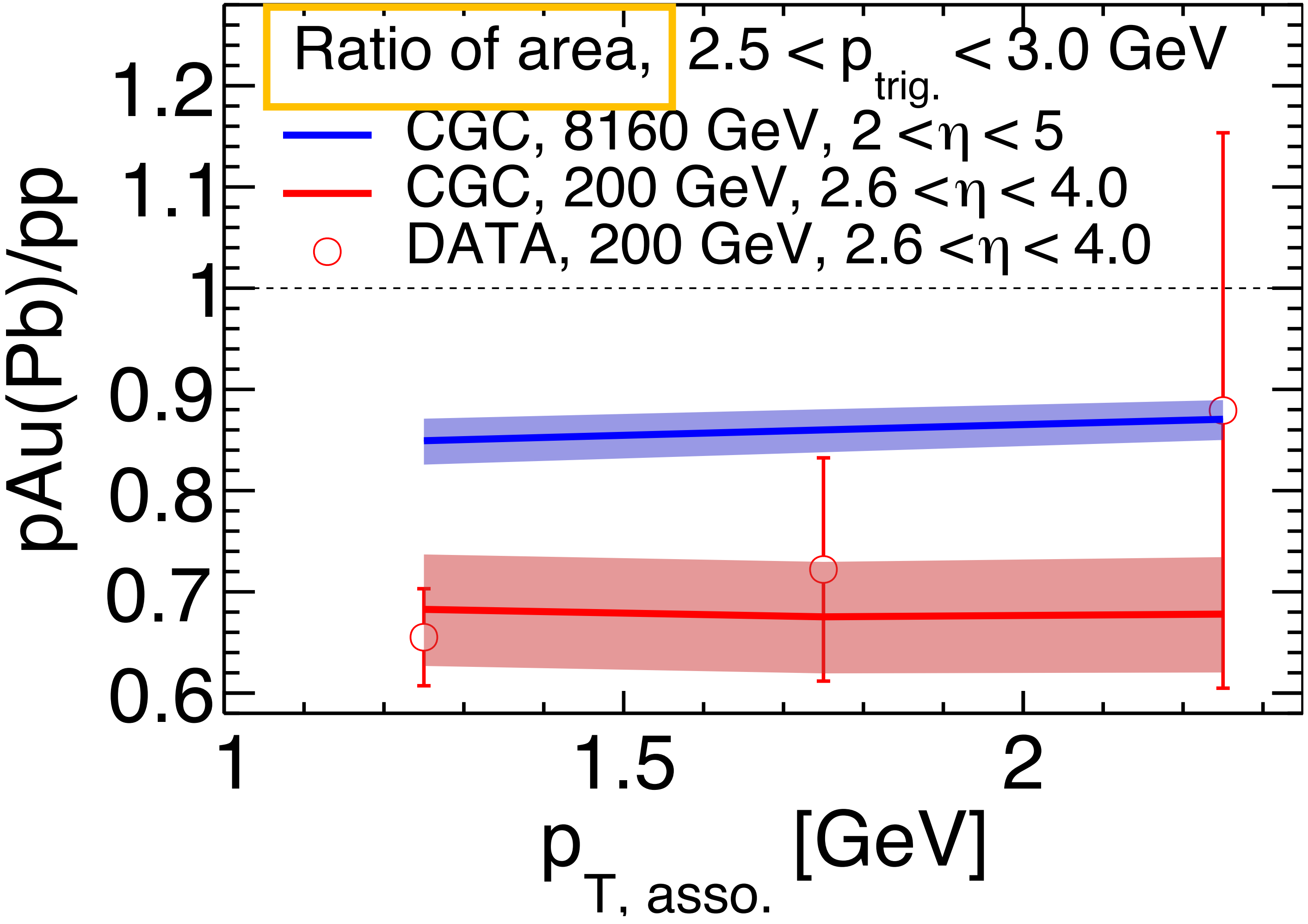

- Surprisingly, LHCb has the **smaller suppression** than STAR, even LHCb has smaller x_g .

$< k_T/Q_s >$ probed by STAR and LHCb

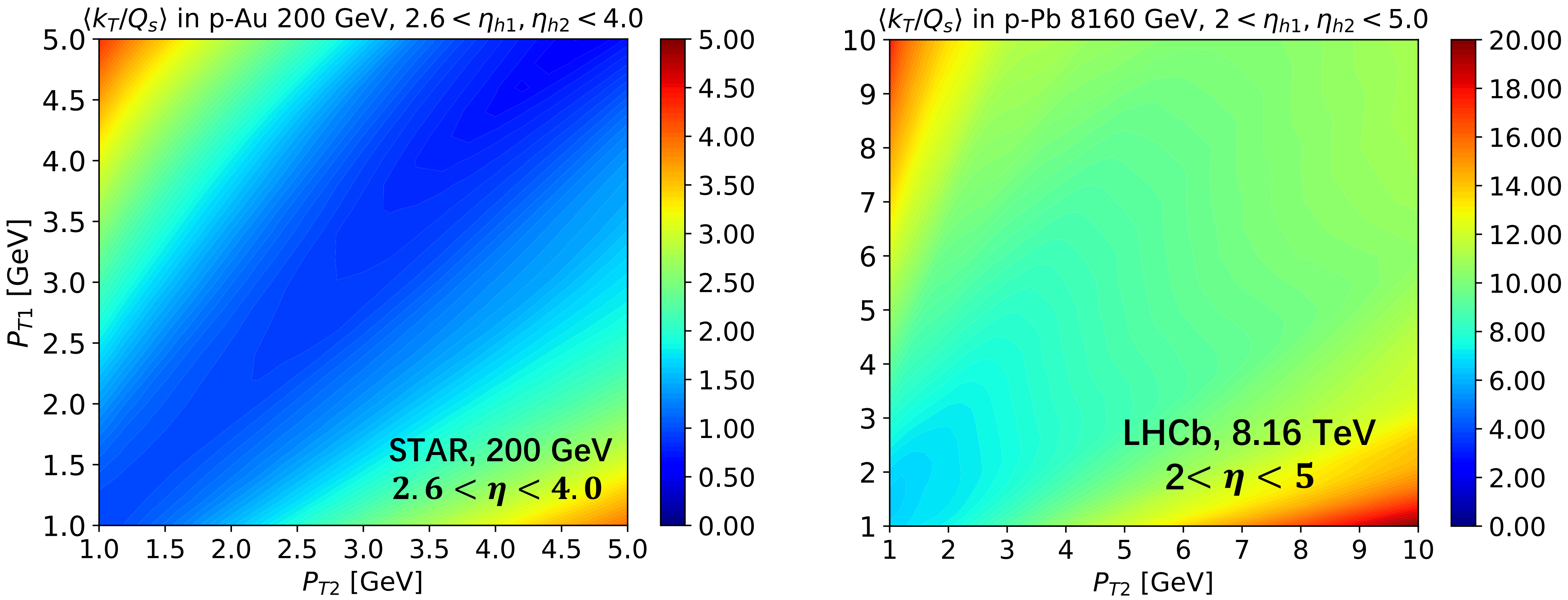

- $< k_T/Q_s >$ probed by di-hadron at **LHCb is much larger than that at STAR**, which partially explains the smaller saturation effects in LHCb than STAR.

Fragmentation fraction probed by STAR and LHCb

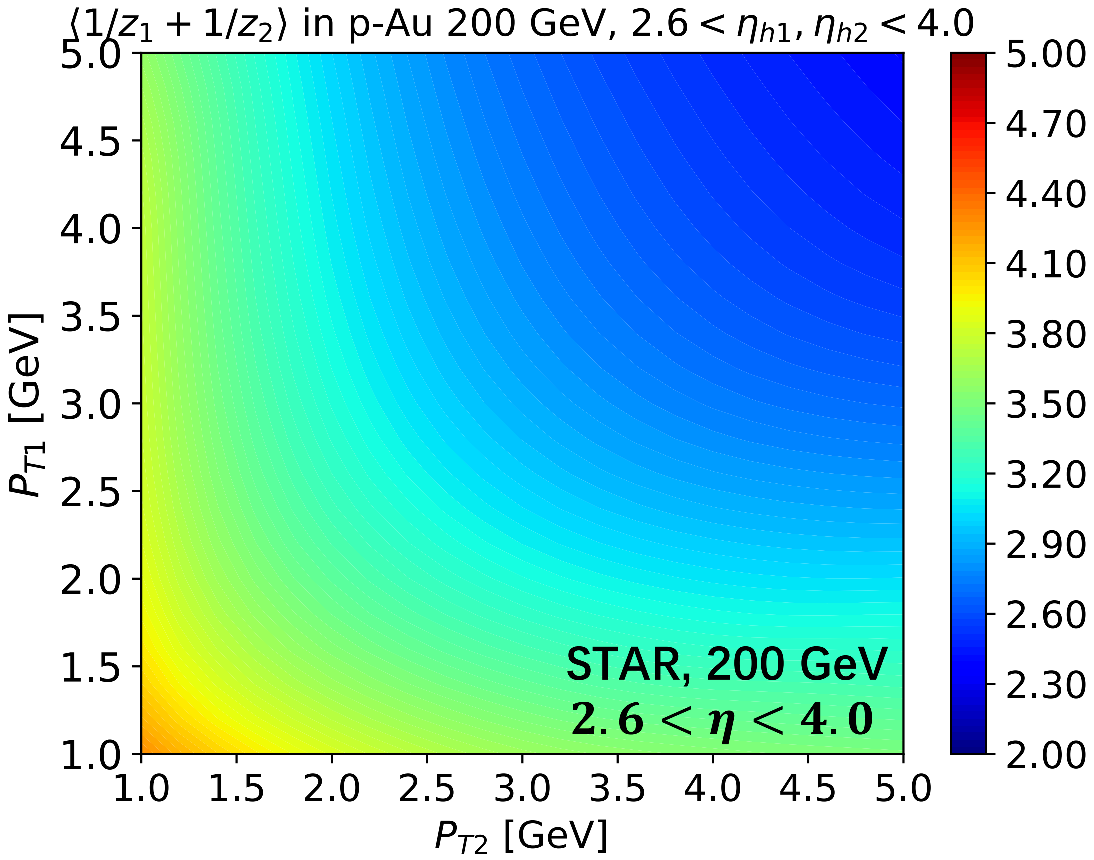

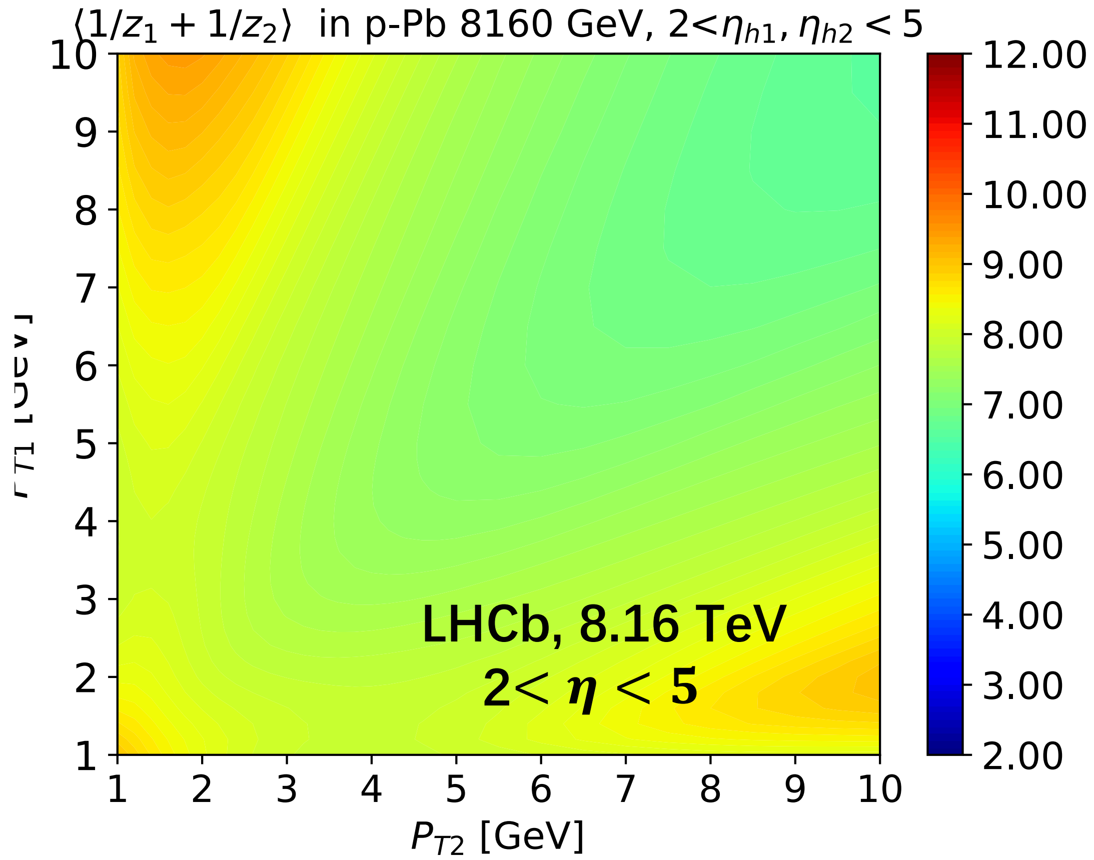

- STAR has much smaller $(1/z_1 + 1/z_2)$, or **larger $< z >$,** than that at LHCb.

NPDF and CGC results

D. V. Perepelitsa, PRC.111.054901

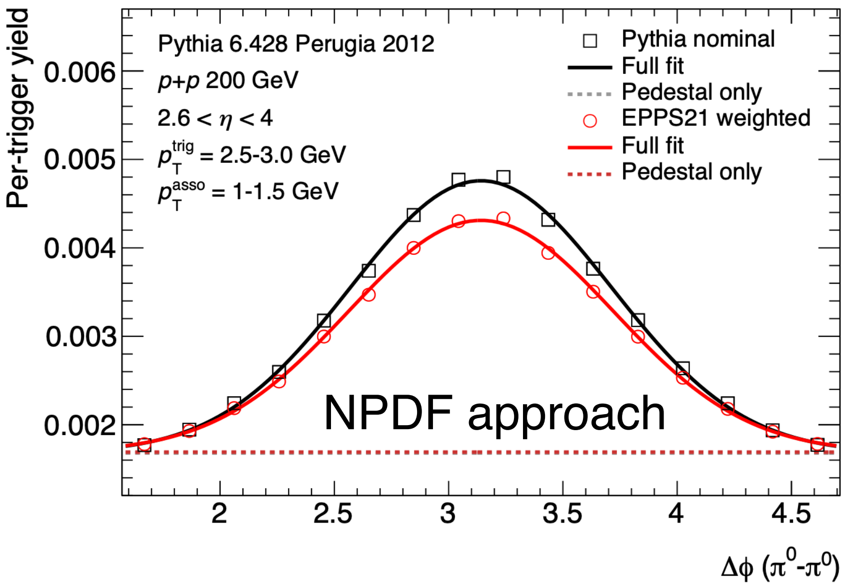

W. Zhao, etc, al., in progress.

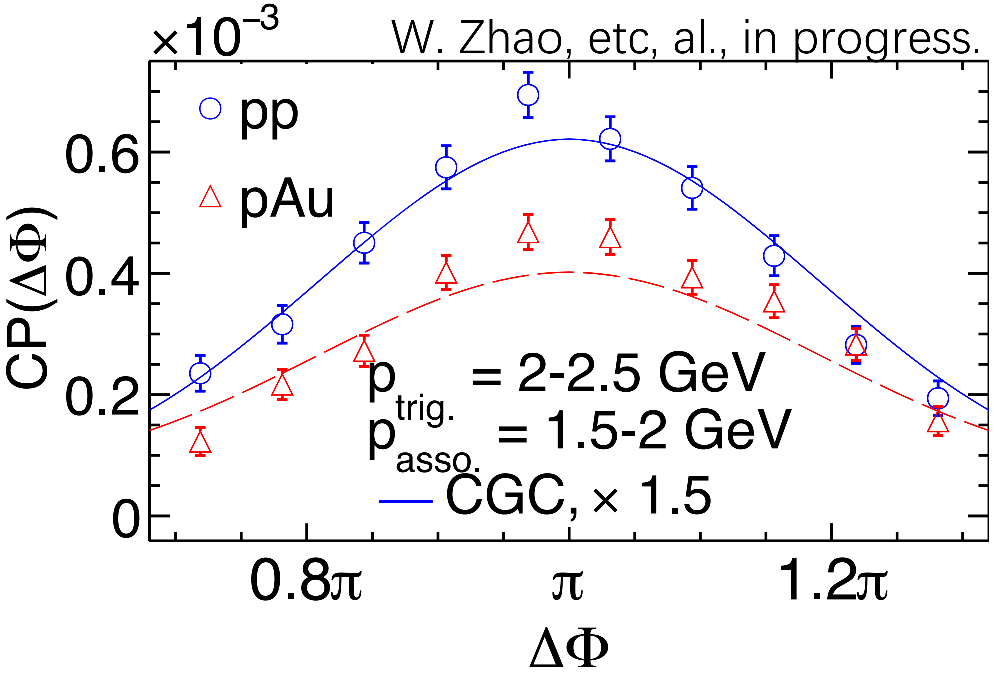

- NPDF and CGC approaches have the similar results.

See also:

- J. L. Albacete and C. Marquet, Phys. Rev. Lett. 105, 162301 (2010)
- T. Lappi and H. Mantysaari, Nucl. Phys. 908, 51-72 (2013).
- van Hameren, etc, al. JHEP 12, 034 (2016).
- A. Stasto, etc. al, Phys. Lett. B 784, 301-306 (2018).
- J. L. Albacete, etc, al. Phys. Rev. D 99, 014002 (2019).

NPDF and CGC results

D. V. Perepelitsa, PRC.111.054901

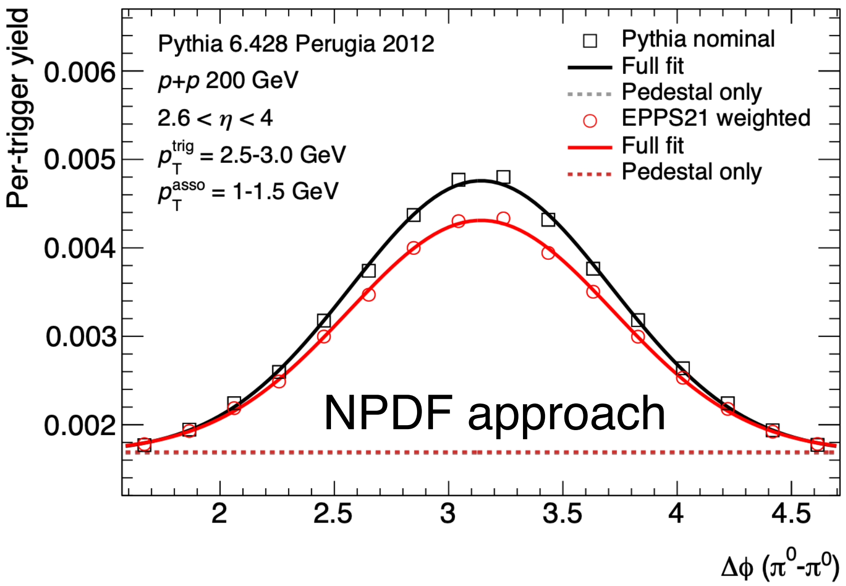

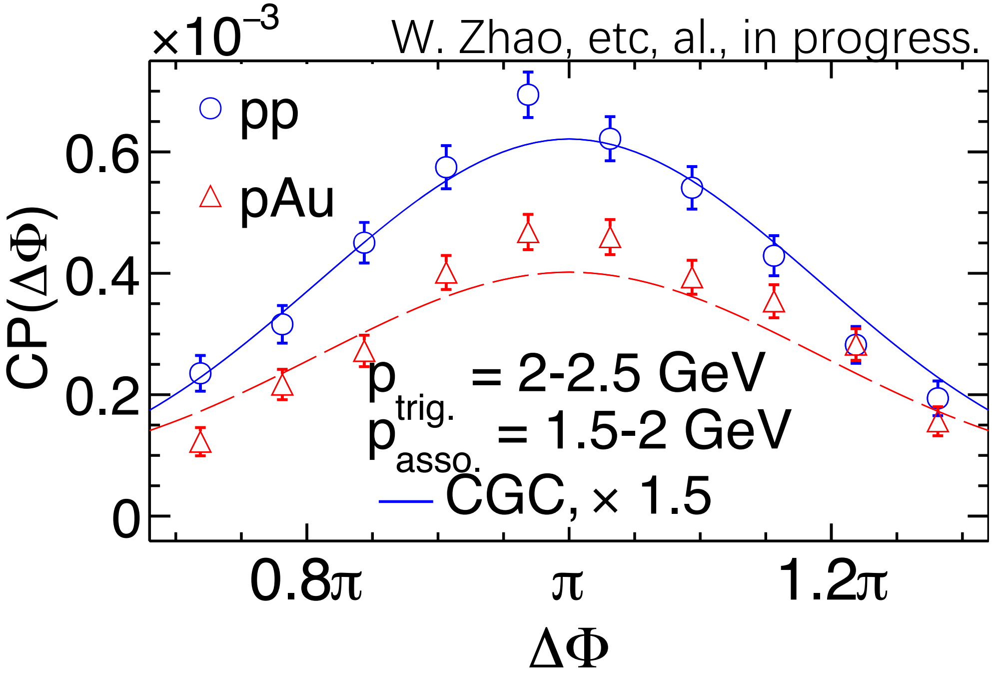

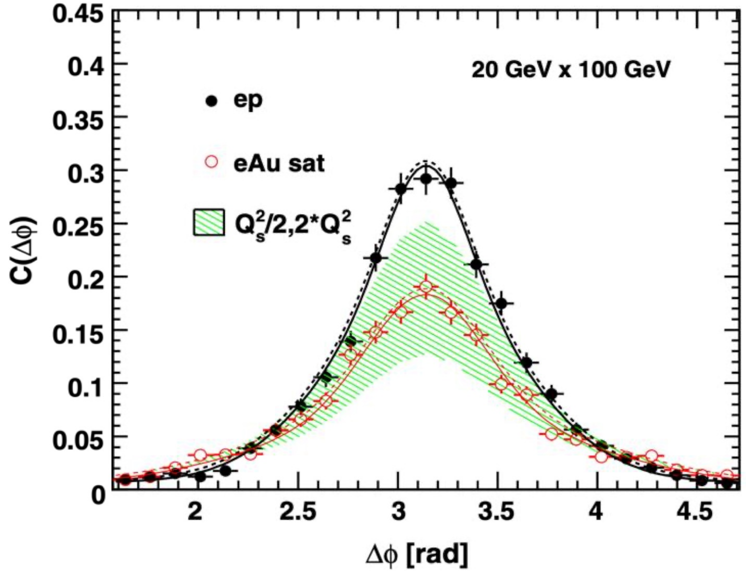

L. Zheng et al., PRD 89 (2014) 074037

- NPDF and CGC approaches have the similar results.
- EIC/UPC provide the **clean environment** for dihadron correlations

See also:

- J. L. Albacete and C. Marquet, Phys. Rev. Lett. 105, 162301 (2010)
- T. Lappi and H. Mantysaari, Nucl. Phys. 908, 51-72 (2013).
- van Hameren, etc, al. JHEP 12, 034 (2016).
- A. Stasto, etc. al, Phys. Lett. B 784, 301-306 (2018).
- J. L. Albacete, etc, al. Phys. Rev. D 99, 014002 (2019).

Summary

- A comprehensive analysis of UPC/DIS and heavy-ion collision data across various energies will provide a precise understanding of **gluon saturation**, the **initial conditions** of heavy-ion collisions, and the **QGP properties**.

- CGC model can reasonably reproduce the STAR dihadron data.
- LHCb has the **less suppressions** of dihadron than that at STAR.
- Heavy flavour, EEC could help.

Thanks for Your Attention!

Back Up

Back Up

Soft gluon resummation

A. H. Mueller, B. W. Xiao and F. Yuan, PhysRevLett.110.082301.

$$\frac{d\sigma}{d^2p_{T1}d^2p_{T2}} \propto \int \frac{d^2b_\perp}{(2\pi)^2} e^{-i\vec{q}_T\cdot\vec{b}_\perp} f(x_1)\otimes F(x_2,b_\perp)\otimes H\otimes e^{-S_{\rm Sudakov}}$$

- Sudakov factors : $S_{\rm Sud}^{a+b\to c+d}(b_\perp) = \sum_{i=a,b,c,d} S_p^i(b_\perp) + \underline{\boldsymbol{C_{np}}}\times \sum_{i=a,c,d} S_{np}^i(b_\perp),$

$$S_p^{q+g\to q+g}(Q,b_\perp) = \int_{\mu_b^2}^{Q^2}\frac{d\mu^2}{\mu^2}\left[2(C_F+C_A)\frac{\alpha_s}{2\pi}\ln\left(\frac{Q^2}{\mu^2}\right) - \left(\frac{3}{2}C_F + C_A\beta_0\right)\frac{\alpha_s}{\pi}\right],$$

$$S_p^{g+g\to g+g}(Q,b_\perp) = \int_{\mu_b^2}^{Q^2}\frac{d\mu^2}{\mu^2}\left[4C_A\frac{\alpha_s}{2\pi}\ln\left(\frac{Q^2}{\mu^2}\right) - 3C_A\beta_0\frac{\alpha_s}{\pi}\right].$$

$$S_{np}^{q+g\to q+g}(Q,b_\perp) = \left(2+\frac{C_A}{C_F}\right)\frac{g_1}{2}b_\perp^2 + \left(2+\frac{C_A}{C_F}\right)\frac{g_2}{2}\ln\frac{Q}{Q_0}\ln\frac{b_\perp}{b_*},$$

$$S_{np}^{g+g\to g+g}(Q,b_\perp) = \frac{3C_A}{C_F}\frac{g_1}{2}b_\perp^2 + \frac{3C_A}{C_F}\frac{g_2}{2}\ln\frac{Q}{Q_0}\ln\frac{b_\perp}{b_*}.$$

Using the b^*-prescription: $\beta_0 = (11-2n_f/3)/12,\ \mu_b = 2e^{-\gamma_E}/b_*,$ and $b_* = b_\perp/\sqrt{1+b_\perp^2/b_{\max}^2}.$

Area ratio and width ratio between pAu and pp

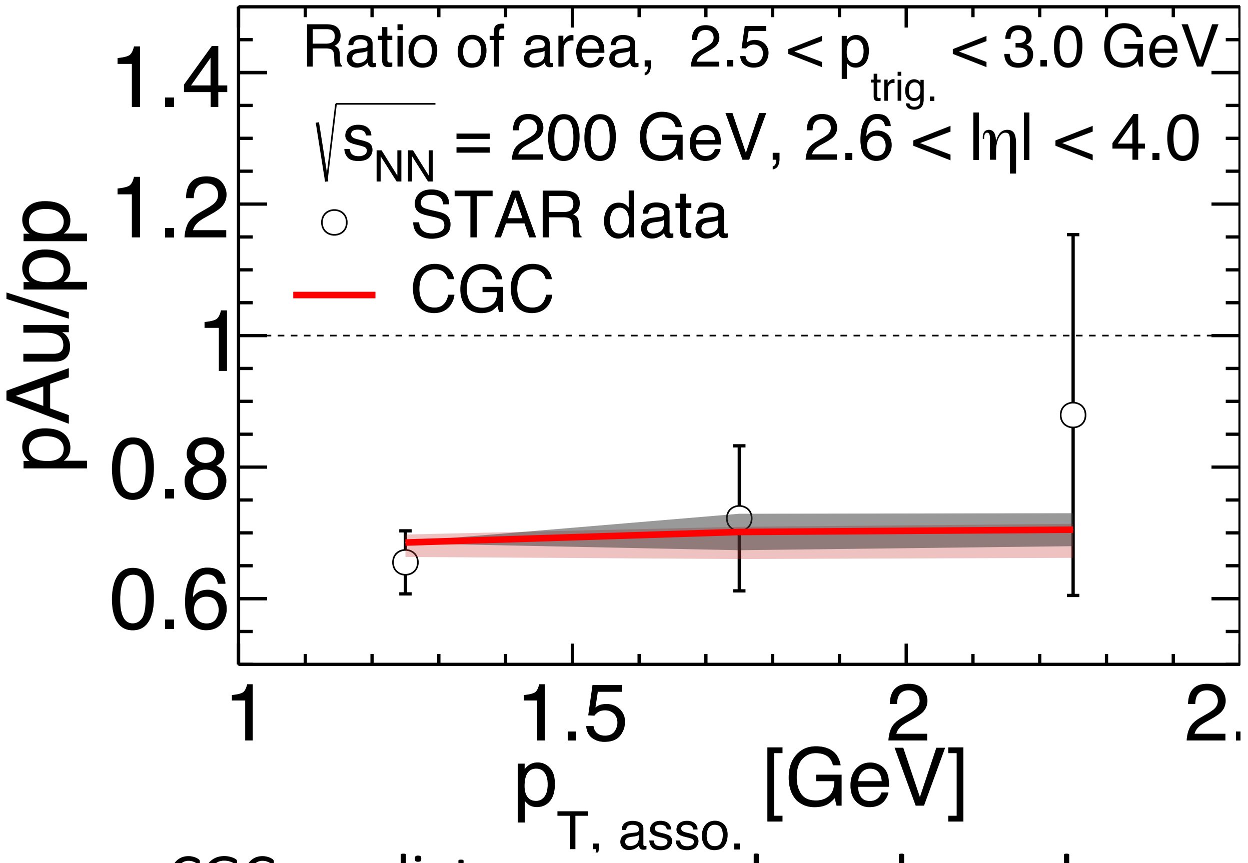

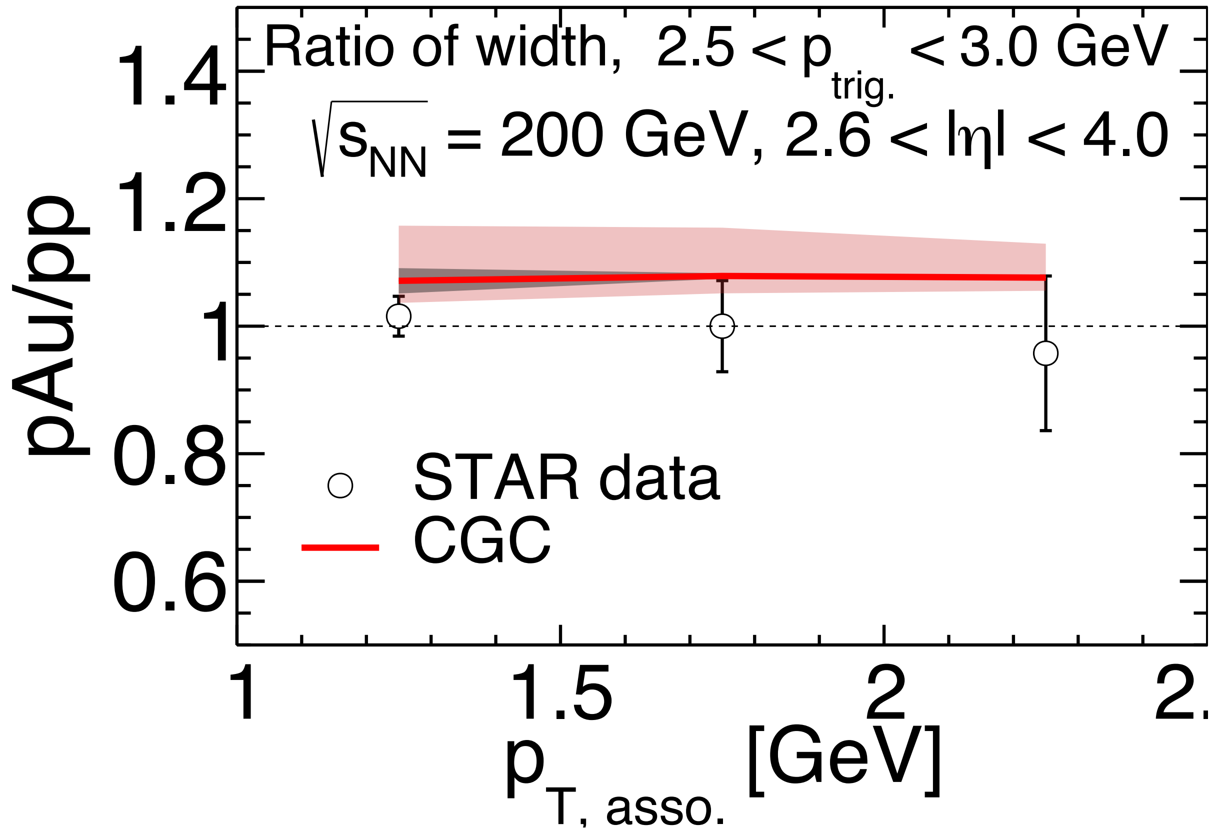

- CGC predicts very week p_T dependence.
- The red band calculated by changing the C_{np} from 0.5 to 1.5; The gray band, changed scale from $0.5 * P_T$ to $1.5 * P_T$

$$S_{\text{Sud}}^{a+b\to c+d}(b_\perp) = \sum_{i=a,b,c,d} S_p^i(b_\perp) + \boldsymbol{C_{np}} \times \sum_{i=a,c,d} S_{np}^i(b_\perp),$$

$CP(\Delta\Phi)$ for different C_{np}

$$S_{\text{Sud}}^{a+b\to c+d}(b_\perp) = \sum S_p^i(b_\perp) + C_{np} \times \sum S_{np}^i(b_\perp),$$

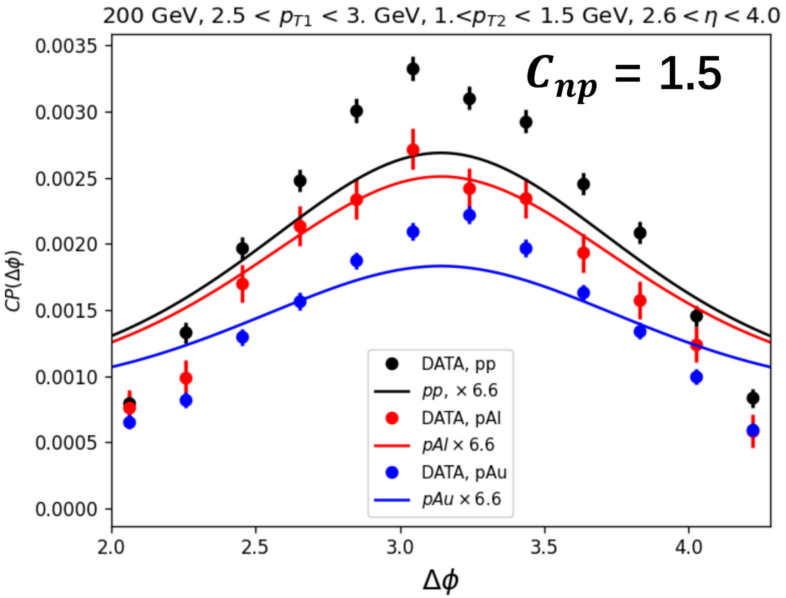

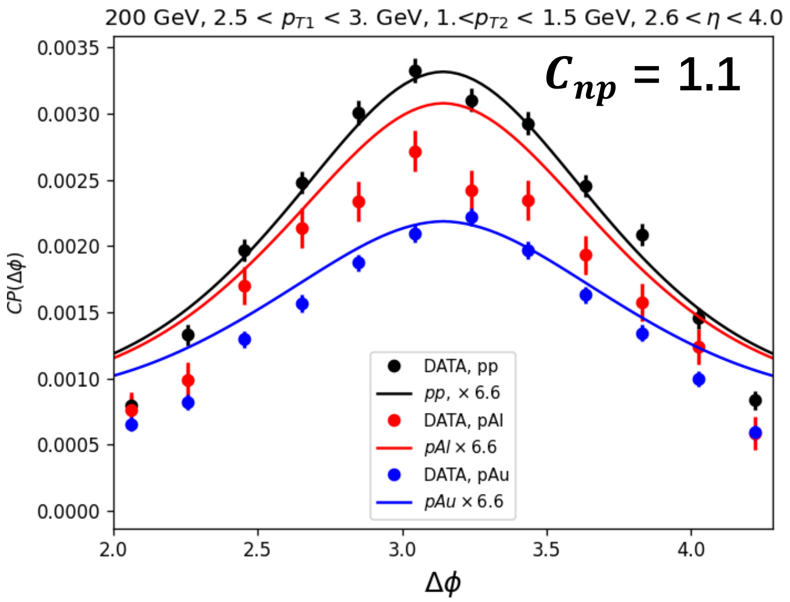

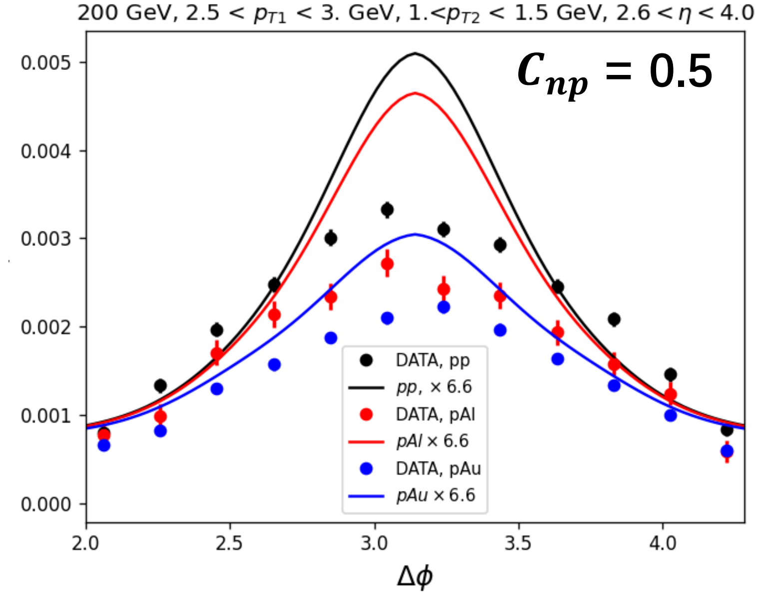

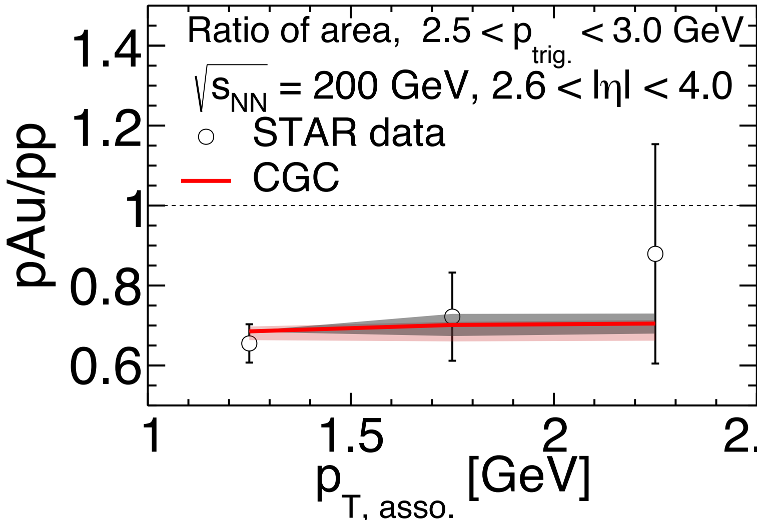

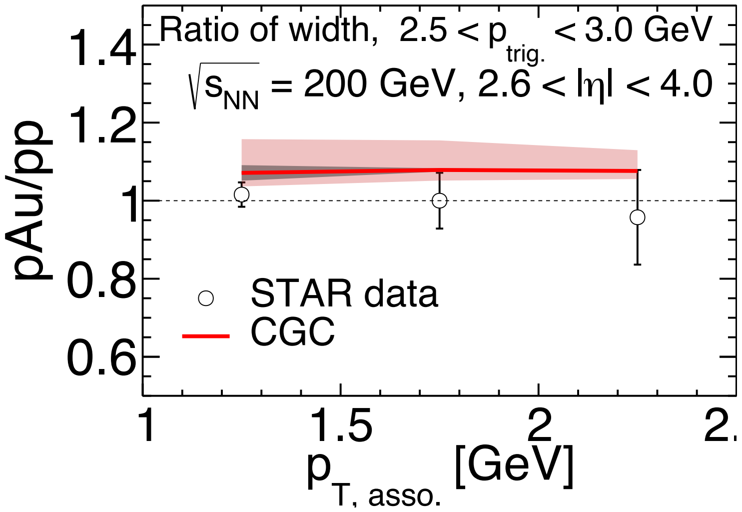

Why asymmetric bins not so good?

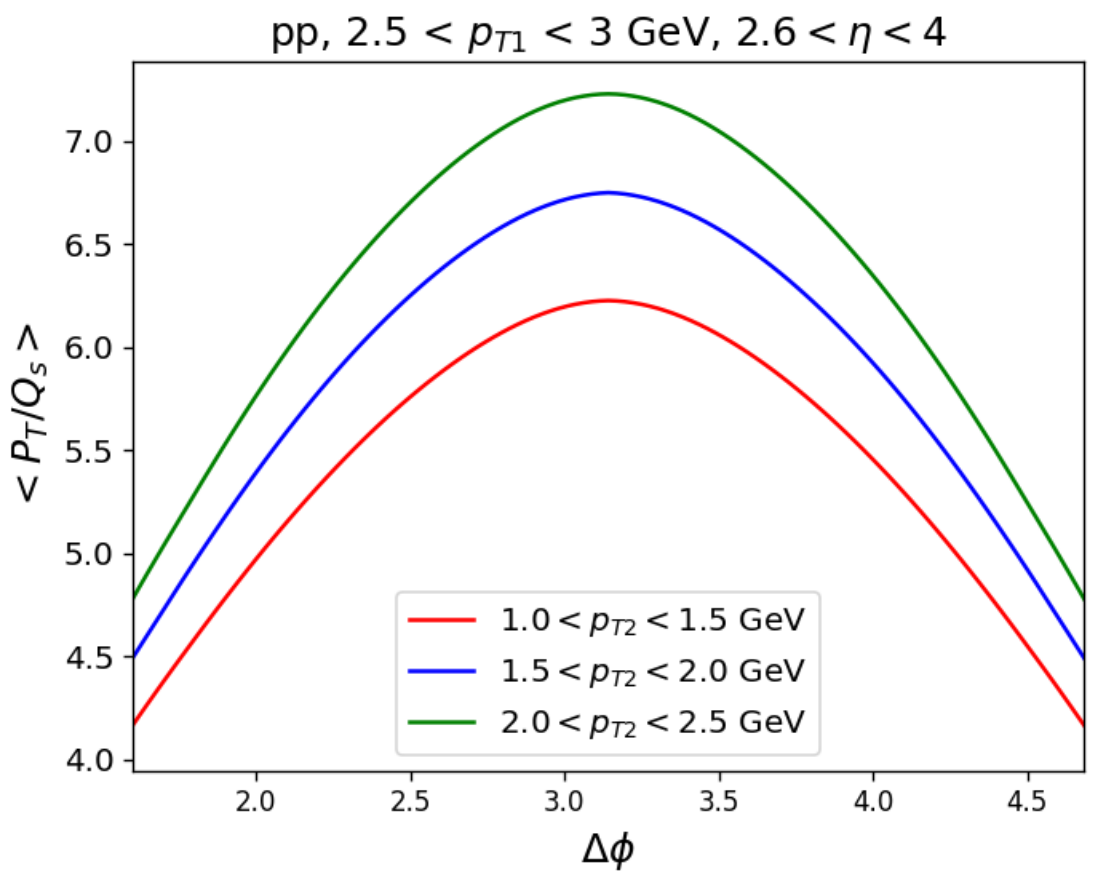

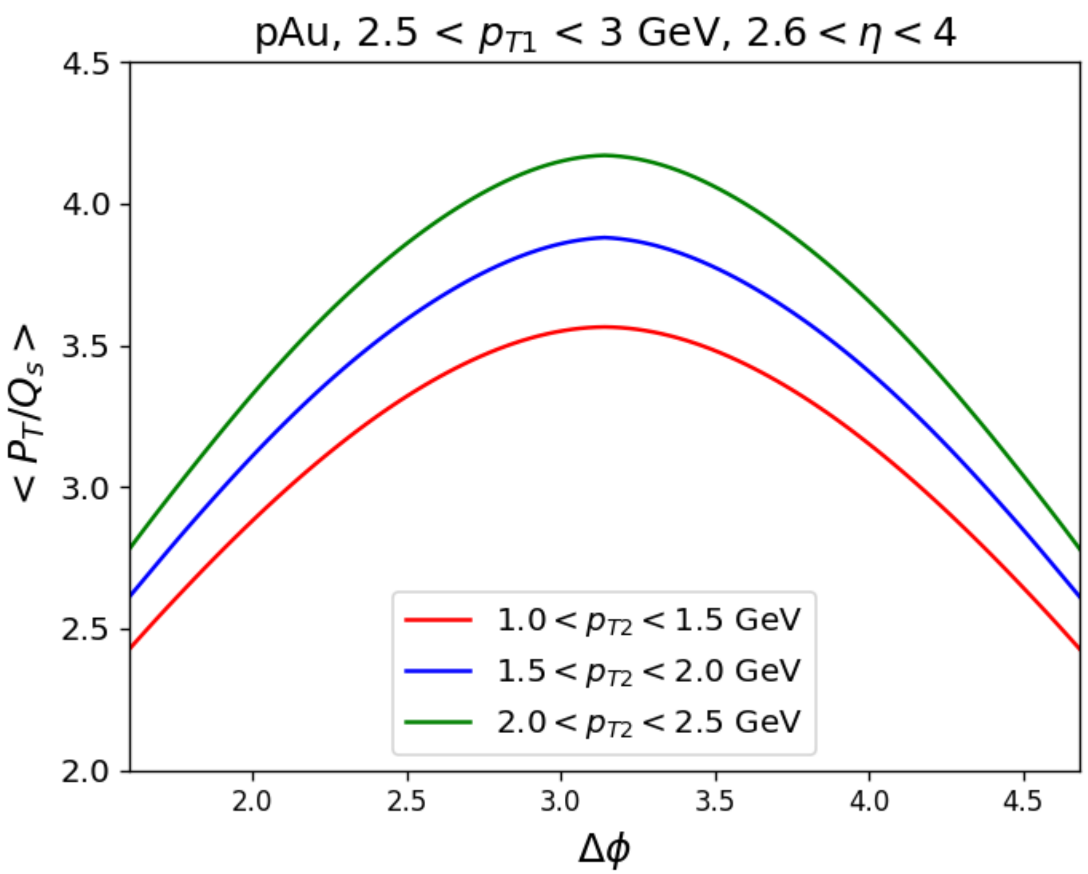

$$P_t = (1-z)p_{1t} - zp_{2t}$$

- Partially because $< P_T/Q_s >$ is not so large in pAu at asymmetric bins.
- How to estimate this model uncertainty when P_T/Q_s is not so large.

Energy evolution to smaller x

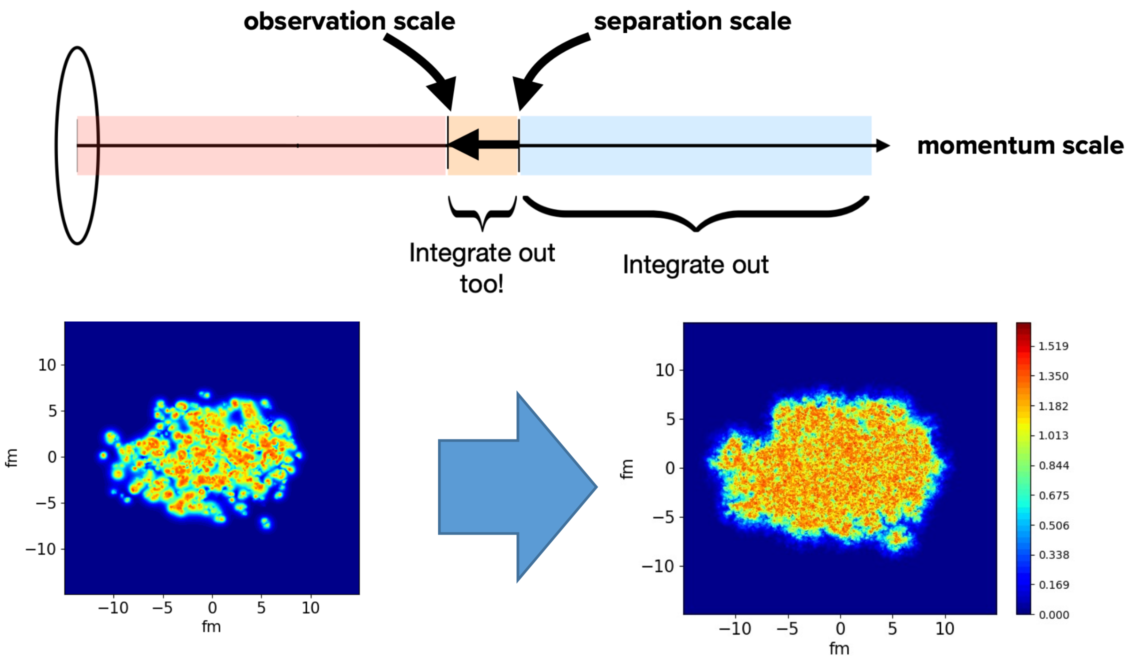

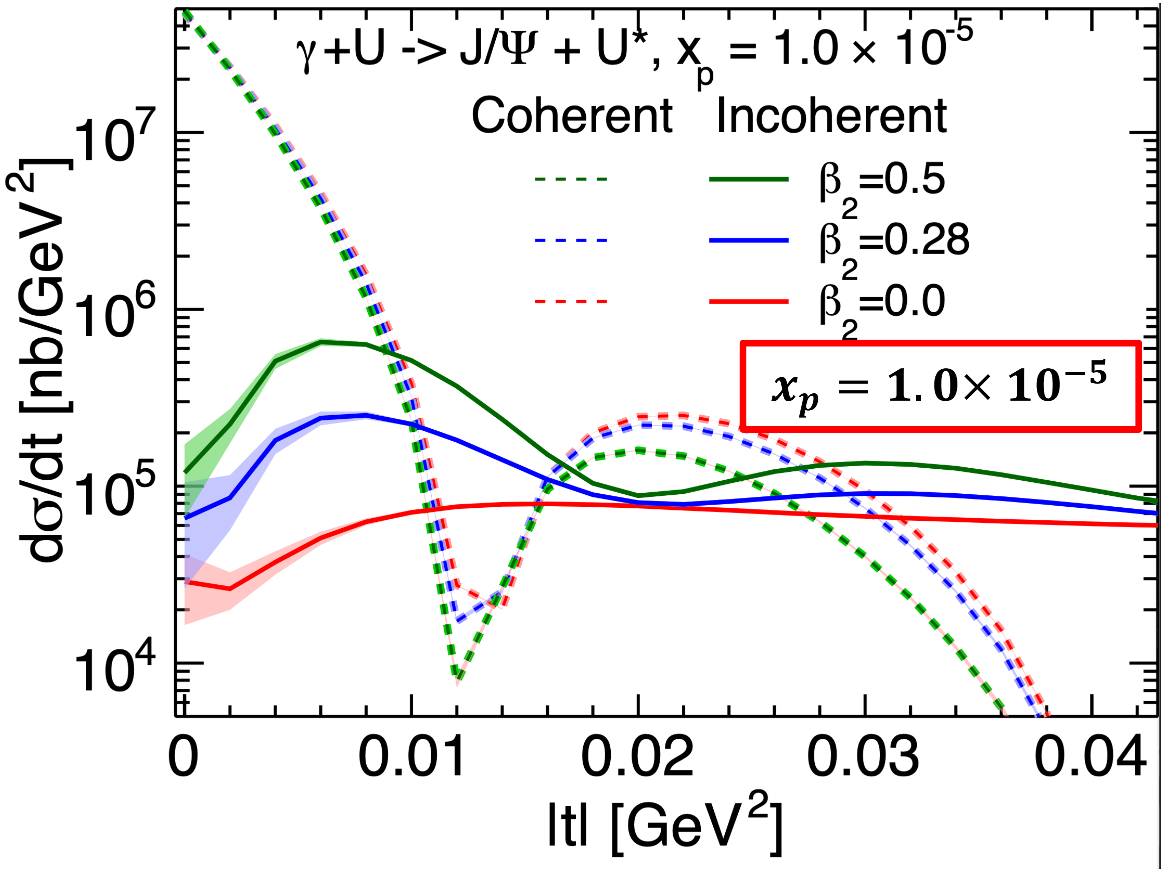

- Energy evolution doesn't wash out this effects.

H.Mantysaari, B.Schenke, C. Shen and W. Zhao PhysRevLett.131.062301.
H.Mantysaari, B.Schenke PRD, 98, 034013.
T. Lappi and H. Mantysaari, EPJC 73, 2307 (2013).
Yuri V. Kovchegov, QUANTUM CHROMODYNAMICS A T HIGH ENERGY

TMD gluon distributions

$$\alpha_s \mathcal{F}_{qg}^{(1)}(\boldsymbol{k}_\perp, x) = \frac{N_c S_\perp}{2\pi^2} \int \frac{r_\perp \mathrm{d}r_\perp}{2\pi} J_0(k_\perp r_\perp) \nabla_\perp^2 \left[1 - S(r_\perp, x)\right]$$

$$\alpha_s \mathcal{F}_{qg}^{(2)}(\boldsymbol{k}_\perp, x) = \frac{C_F S_\perp}{2\pi^2} \int \frac{r_\perp \mathrm{d}r_\perp}{2\pi} J_0(k_\perp r_\perp) \mathcal{K}(r_\perp, x) \left[1 - (S(r_\perp, x))^{N_c/C_F}\right] S(r_\perp, x)$$

$$\alpha_s \mathcal{F}_{gg}^{(1)}(\boldsymbol{k}_\perp, x) = \frac{N_c S_\perp}{2\pi^2} \int \frac{r_\perp \mathrm{d}r_\perp}{2\pi} J_0(k_\perp r_\perp) S(r_\perp, x) \nabla_\perp^2 \left[1 - S(r_\perp, x)\right]$$

$$\alpha_s \mathcal{F}_{gg}^{(2)}(\boldsymbol{k}_\perp, x) = \alpha_s \mathcal{F}_{gg}^{(1)}(\boldsymbol{k}_\perp, x) - \alpha_s \mathcal{F}_{adj}(\boldsymbol{k}_\perp, x)$$

$$\alpha_s \mathcal{F}_{gg}^{(3)}(\boldsymbol{k}_\perp, x) = \frac{C_F S_\perp}{2\pi^2} \int \frac{r_\perp \mathrm{d}r_\perp}{2\pi} J_0(k_\perp r_\perp) \mathcal{K}(r_\perp, x) \left[1 - (S(r_\perp, x))^{N_c/C_F}\right] (S(r_\perp, x))^2$$

$$\alpha_s \mathcal{F}_{adj}(\boldsymbol{k}_\perp, x) = \frac{C_F S_\perp}{2\pi^2} \int \frac{r_\perp \mathrm{d}r_\perp}{2\pi} J_0(k_\perp r_\perp) \nabla_\perp^2 \left[1 - (S(r_\perp, x))^{N_c/C_F}\right]$$

- Here we use the Gaussian approximation: $S(\boldsymbol{x}_\perp, \boldsymbol{y}_\perp, x) = \frac{1}{N_c} \langle \mathrm{Tr}\left[V(\boldsymbol{x}_\perp) V^\dagger(\boldsymbol{y}_\perp)\right] \rangle_x$

  Assume translational invariance: $S(|\boldsymbol{x}_\perp - \boldsymbol{y}_\perp|, x) = \frac{1}{N_c} \langle \mathrm{Tr}\left[V(\boldsymbol{x}_\perp) V^\dagger(\boldsymbol{y}_\perp)\right] \rangle_x$

  Mean-field approximation: $\langle \mathrm{Tr}\left[\mathcal{O}_1\right] \mathrm{Tr}\left[\mathcal{O}_2\right] \rangle_x = \langle \mathrm{Tr}\left[\mathcal{O}_1\right] \rangle_x \langle \mathrm{Tr}\left[\mathcal{O}_2\right] \rangle_x$

Initial conditions for rcBK

- The dipole-nucleus amplitude is obtained by solving the rcBK evolution equation.
- The initial conditions at $x_0 = 0.01$ is model by parametrization, based on McLerran-Venugopalan model

$$\mathcal{N}(\mathbf{r}_T) = 1 - \exp\left[-\frac{(\mathbf{r}_T{}^2 Q_{s0}^2)^\gamma}{4} \ln\left(\frac{1}{|\mathbf{r}_T|\Lambda_{QCD}} + e_c \cdot e\right)\right]$$

- The BK equation with strong coupling constant α_s as a function of the transverse separation $r = |r_T|$

$$\alpha_s(r) = \frac{12\pi}{(33 - 2N_f)\log\left(\frac{4C^2}{r^2\Lambda_{QCD}^2}\right)},$$

- We use $Q_{p,s0}^2 = 0.168\, GeV^2$, $\gamma = 1.119$, $C = 1.1715$, $\Lambda_{QCD} = 0.24\, GeV$, $e_c = 1$.
- For nucleus, we set $Q_{Al,s0}^2 = 1.2\, Q_{p,s0}^2$; $Q_{Au,s0}^2 = 2.75\, Q_{p,s0}^2$; $Q_{Pb,s0}^2 = 2.84\, Q_{p,s0}^2$

J. L. Albacete, N. Armesto, J. G. Milhano, P. Quiroga-Arias and C. A. Salgado, Eur. Phys. J. C71 (2011) 1705. (AAMQS collaboration)
F. Deganutti, C. Royon and S. Schlichting, JHEP 01(2024)159.

Some TMDs

- The dipole-nucleus amplitude is then obtained by solving the rcBK evolution equation.

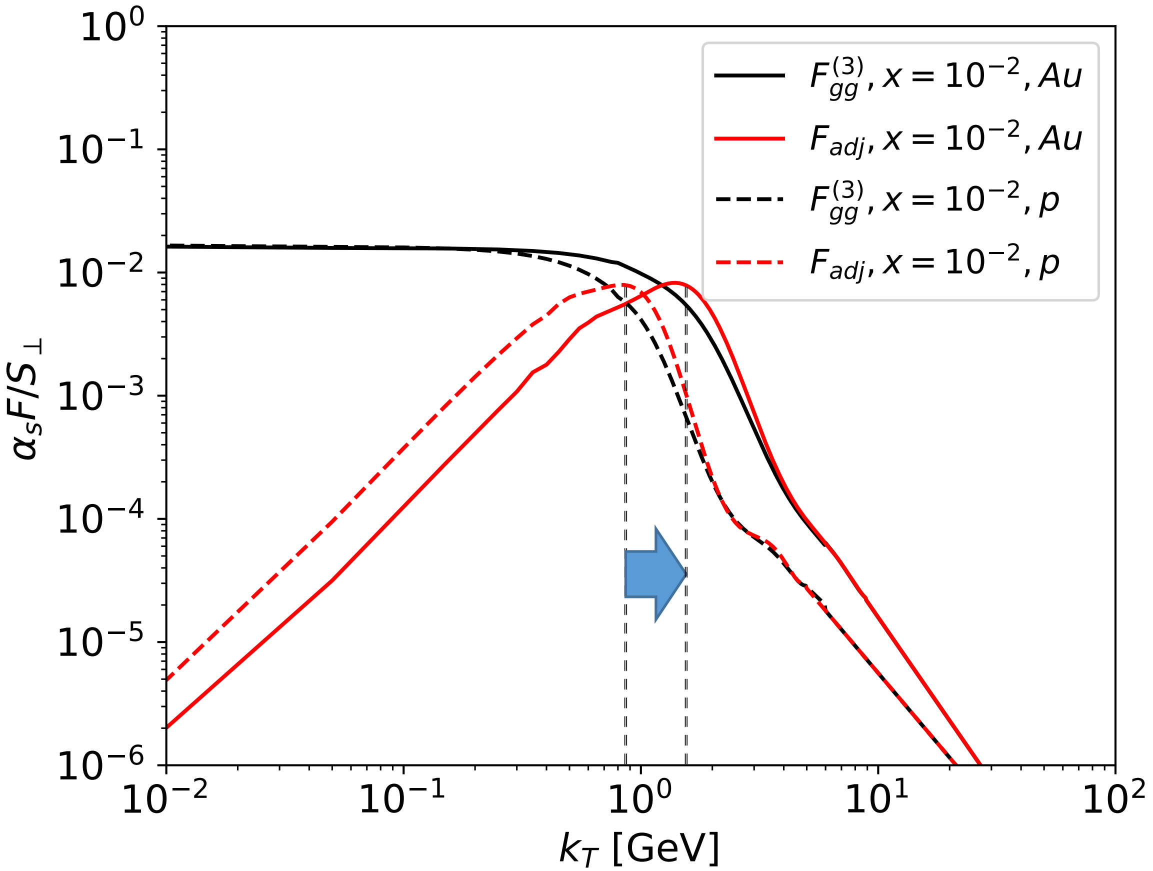

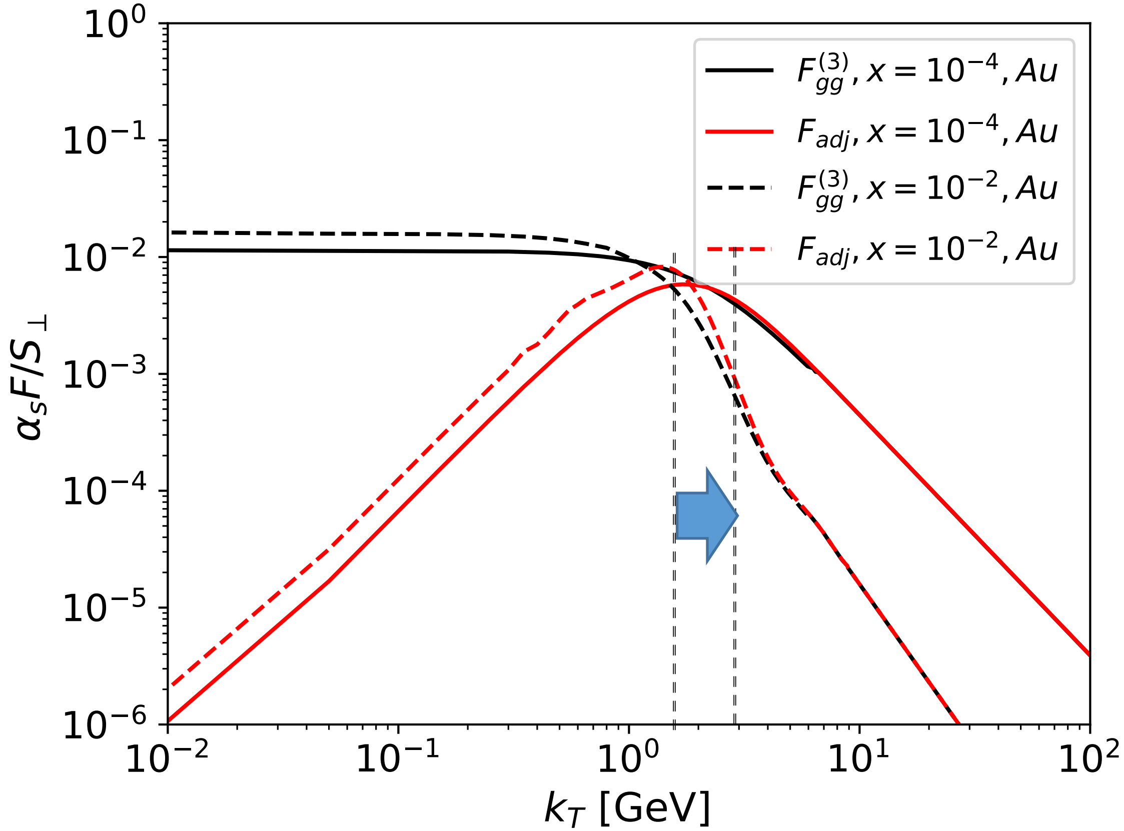

- Saturation scale moves to higher number from proton to nucleus.
- Saturation scale moves to higher number at smaller x_g.

Re-construct 3D profile of polarized light ion

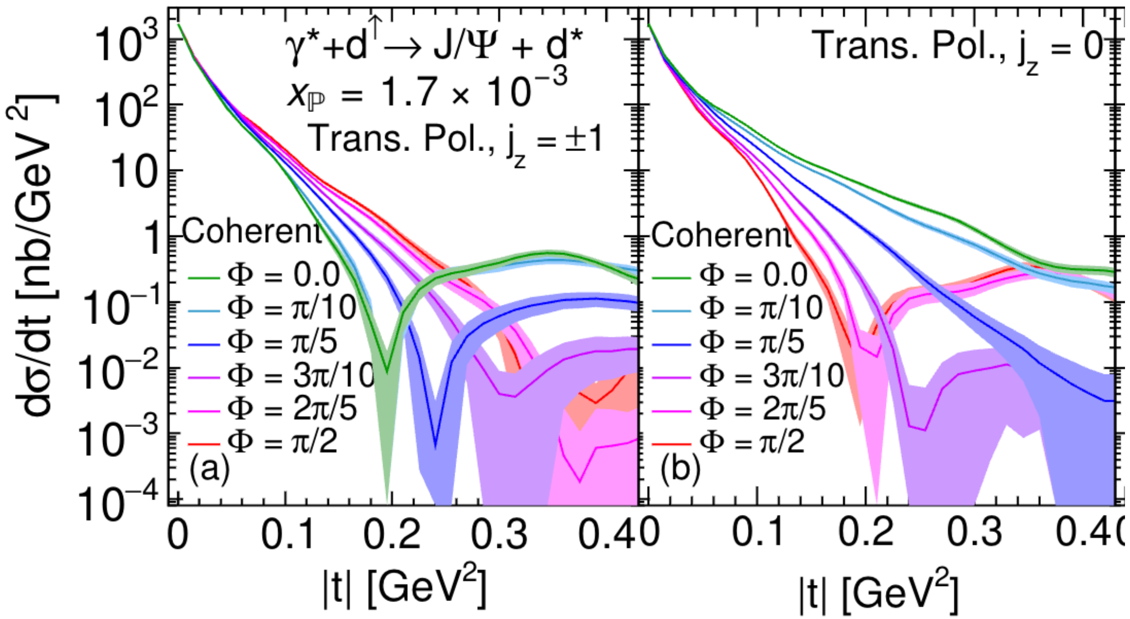

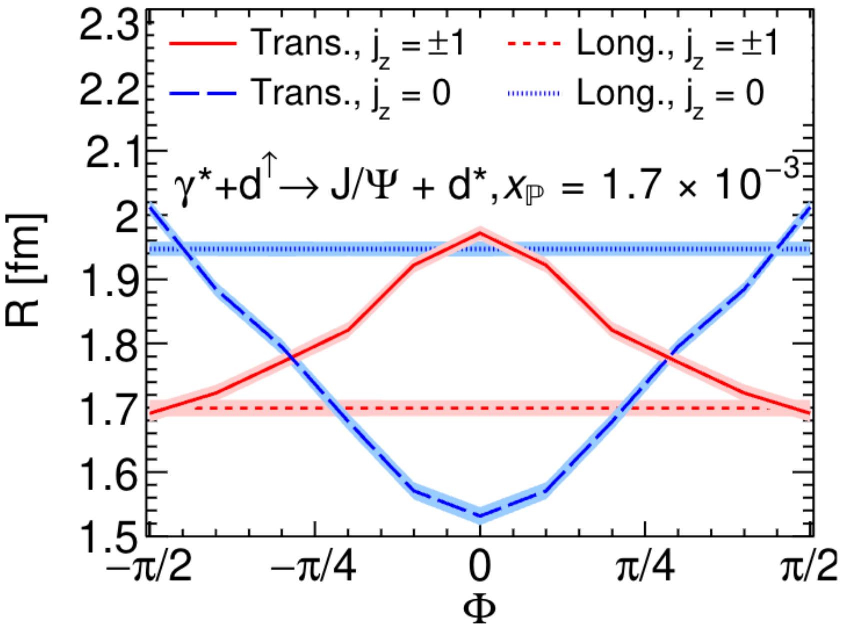

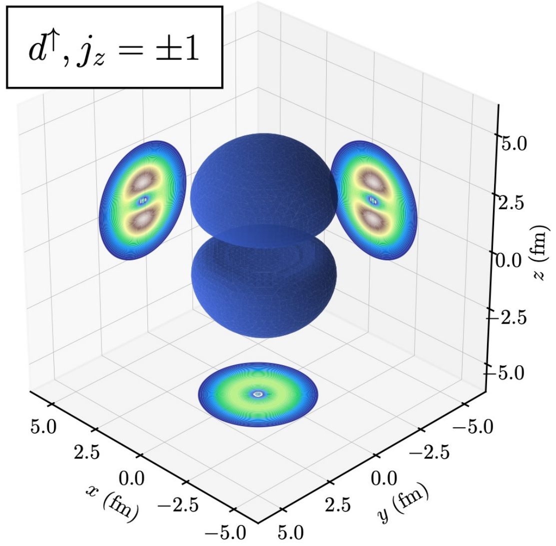

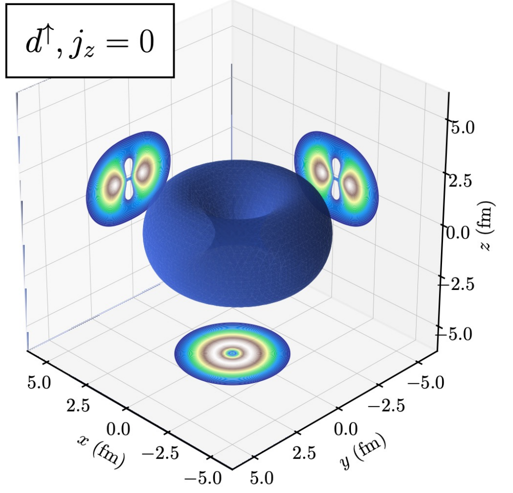

$$d\sigma/dt \sim e^{-B_D|t|} \quad R = \sqrt{2B_D}.$$

- Re-construct the **3D nucleon density profile** of the polarized light nuclei.

H. Mäntysaari, F. Salazar, B.Schenke, C. Shen and W. Zhao, PLB.2024.139053.
P. Bozek and W. Broniowski, PRL.121.202301.

Energy evolution to smaller x

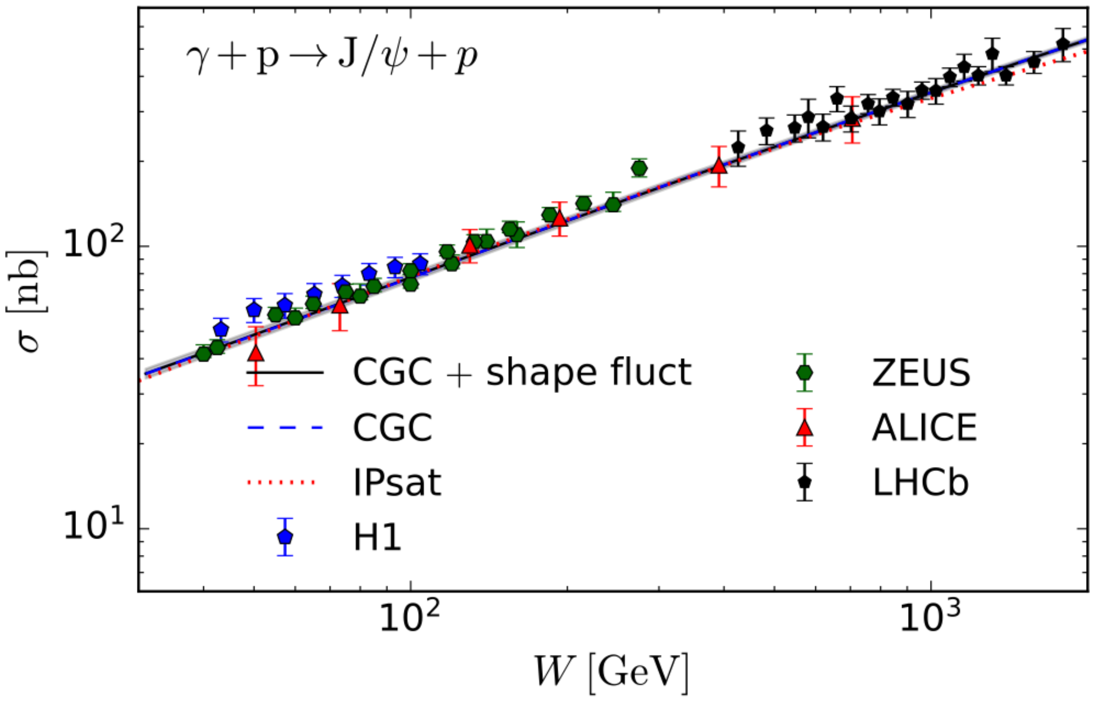

H. Mantysaari, F. Salazar and B. Schenke, Phys. Rev. D 106, no.7, 074019 (2022)

Effects of energy evolution on small systems

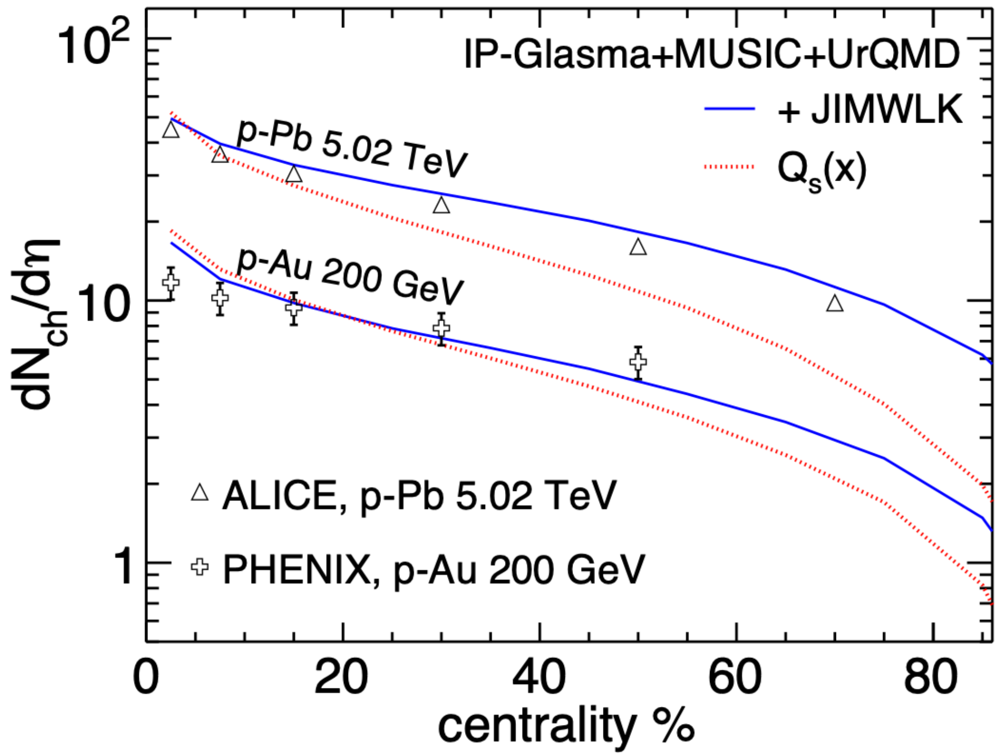

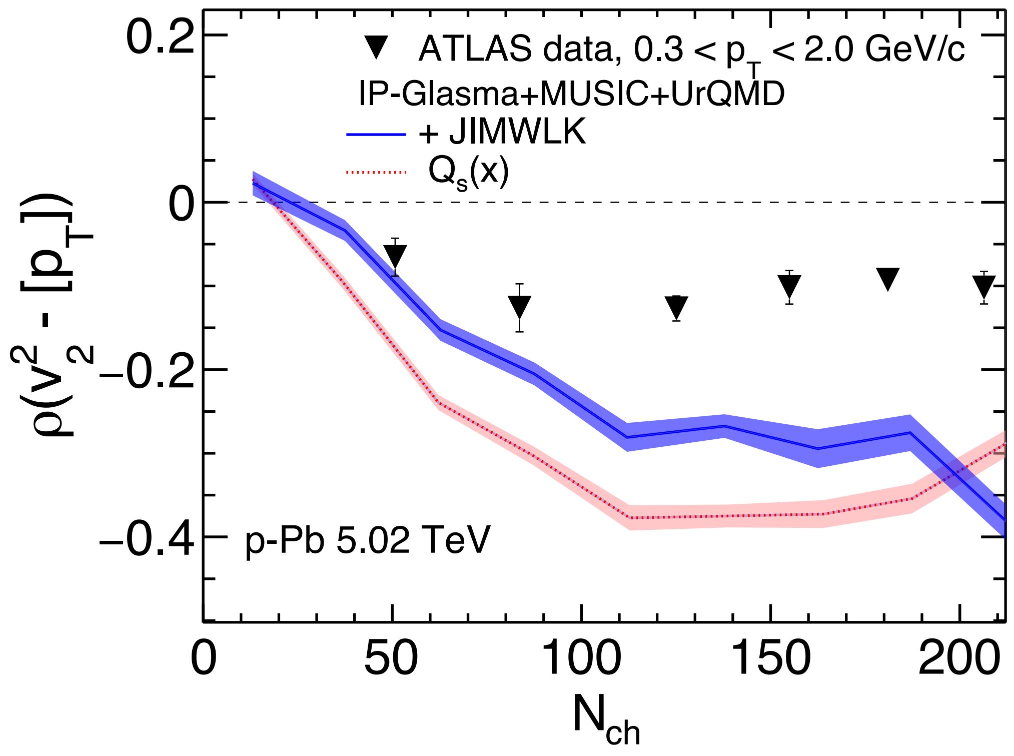

Cite Isabella Danhoni, Aleksas Mazeliauskas

+ JIMWLK: CGC + energy evolution + Hydrodynamics

$\boldsymbol{Q_s(x)}$: CGC (change the $Q_s(x)$ only for different energies) + Hydrodynamics

H. Mäntysaari, B. Schenke, C, Shen and W. Zhao, Phys. Rev. Lett. 135, 022302 (2025)

Probing nucleon at different resolutions

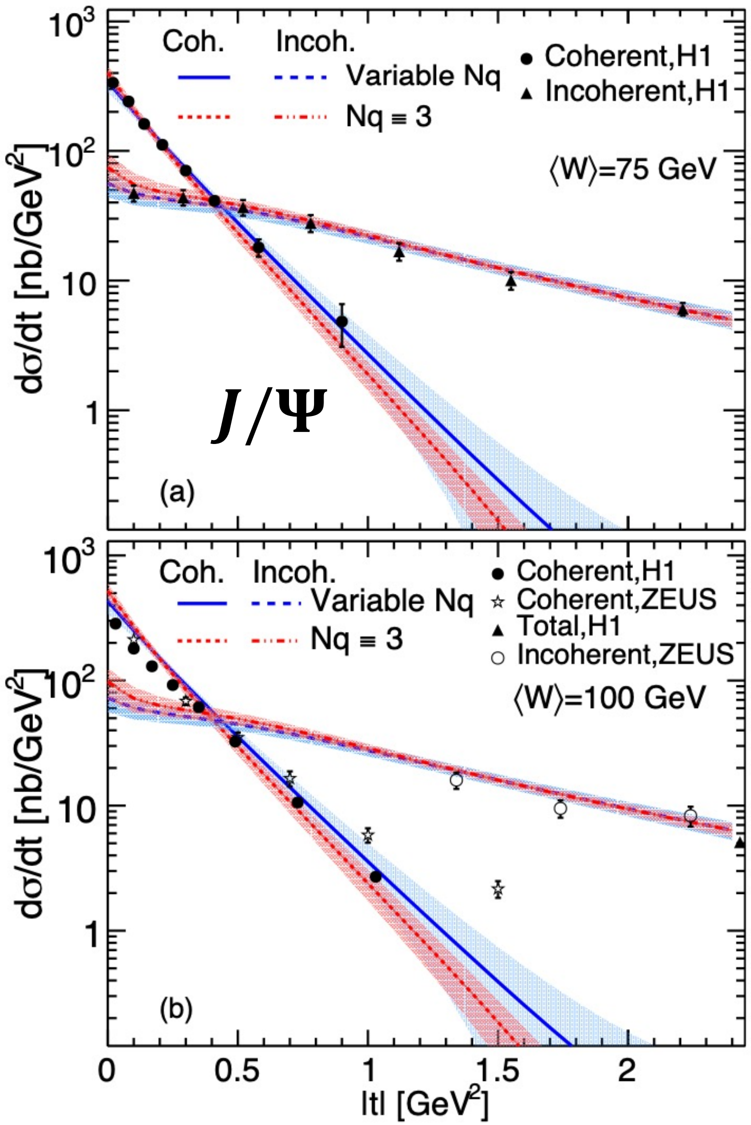

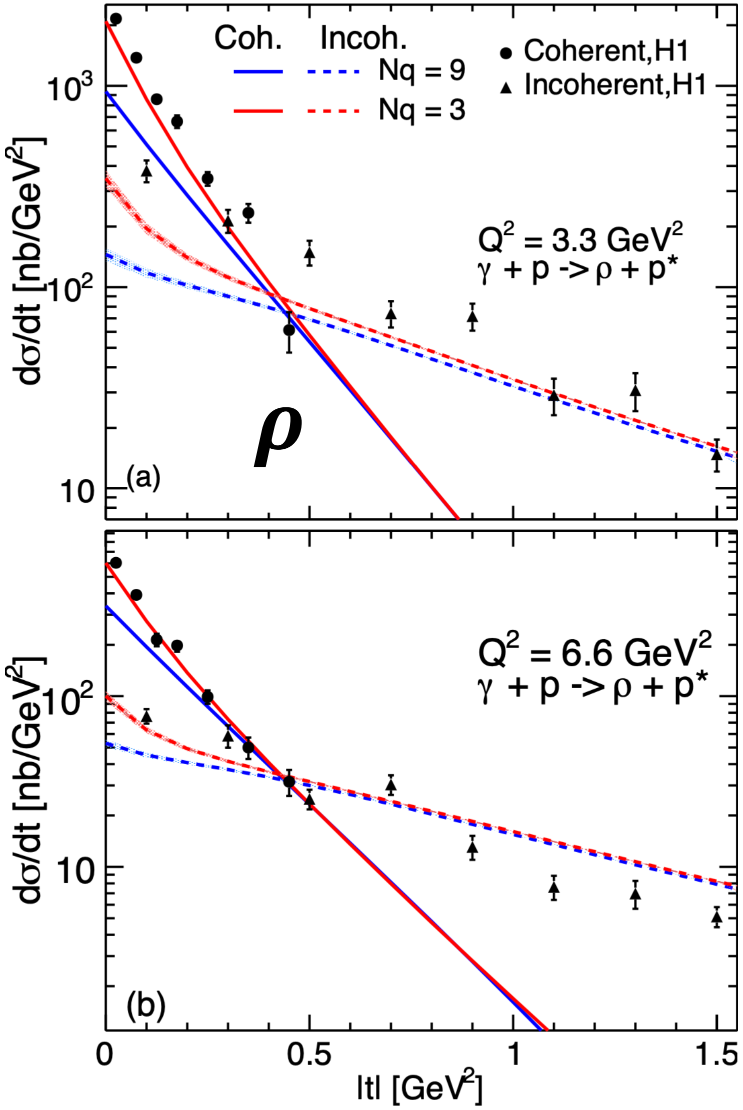

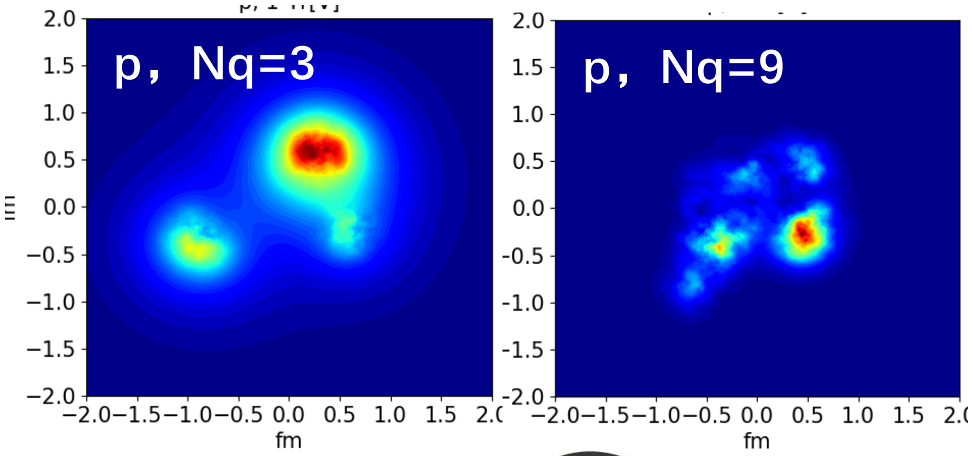

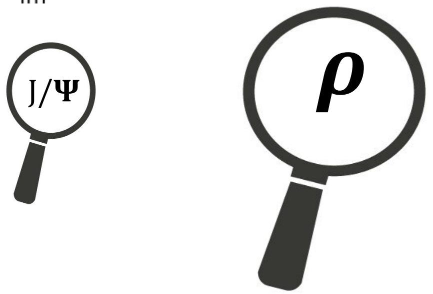

- The ρ mesons probe proton fluctuations at large length scales.
- Sizeable differences observed for ρ productions between Nq=3 and Nq=9 MAPs.

H. Mantysaari, B.Schenke, C. Shen and W. Zhao, Phys. Lett. B 833 (2022), 137348, and in progress.

Determine the Reaction Plane

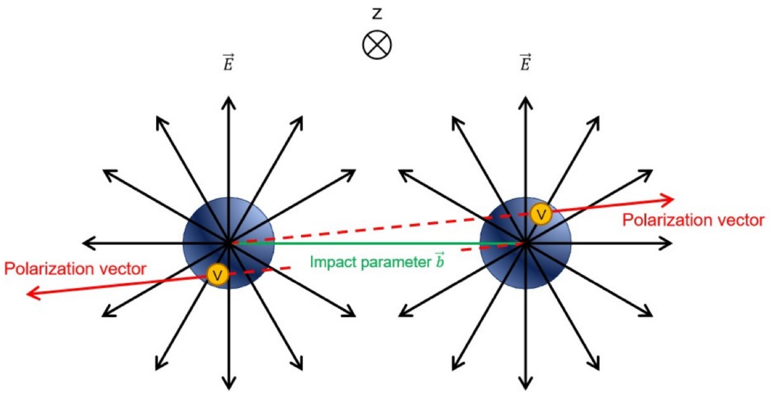

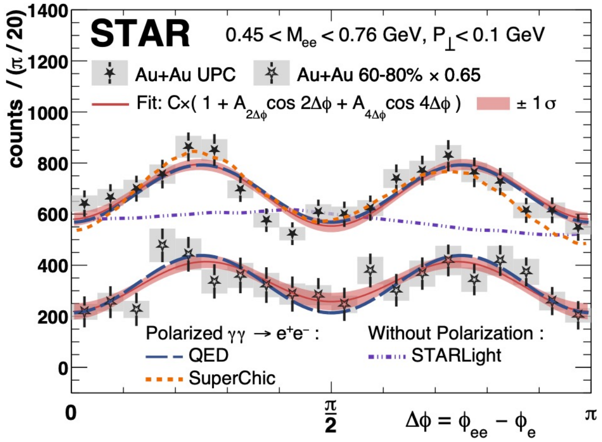

STAR: PhysRevLett.127.052302;

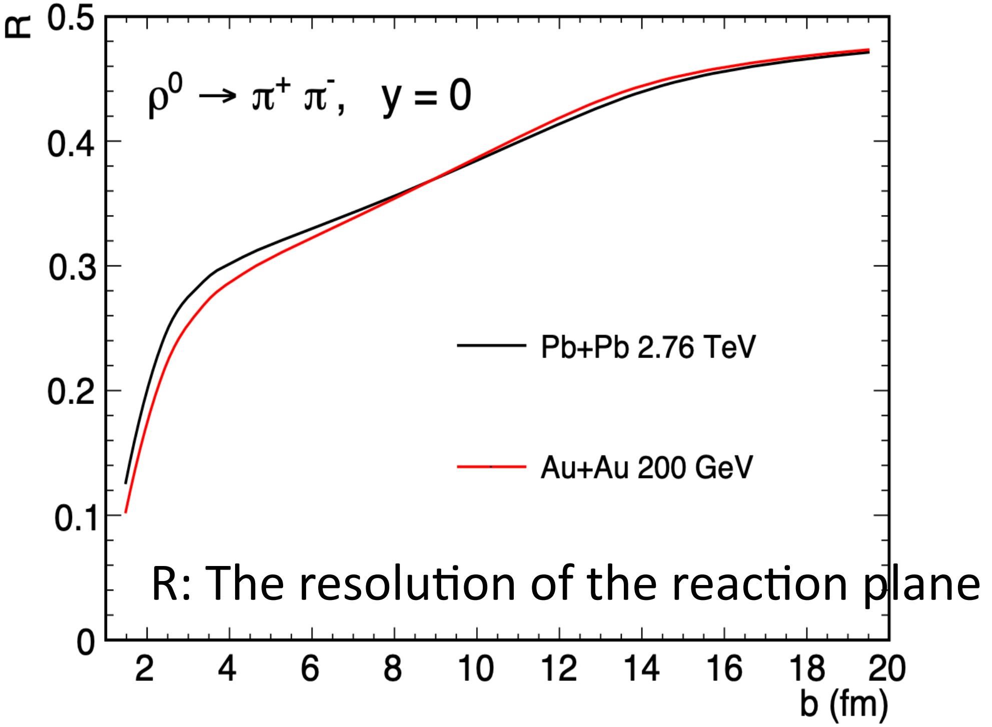

X. Wu, X. Li, Z. Tang, P. Wang and W. Zha, Phys. Rev. Res. 4, no.4, L042048 (2022)

- Photoproduction in HICs is linearly polarized.
- Probe the reaction plane via the feature of linear polarization of the coherent photoproduction process in HICs. -> Connections to the collective flow studying.
- Connections to the collective flow studying.

B-dependence at 0-1% and 0-0.1%